Copyright Warning & Restrictions

The copyright law of the United States (Title 17, United States Code) governs the making of photocopies or other reproductions of copyrighted material.

Under certain conditions specified in the law, libraries and archives are authorized to furnish a photocopy or other reproduction. One of these specified conditions is that the photocopy or reproduction is not to be "used for any purpose other than private study, scholarship, or research." If a, user makes a request for, or later uses, a photocopy or reproduction for purposes in excess of "fair use" that user may be liable for copyright infringement,

This institution reserves the right to refuse to accept a copying order if, in its judgment, fulfillment of the order would involve violation of copyright law.

Please Note: The author retains the copyright while the New Jersey Institute of Technology reserves the right to distribute this thesis or dissertation

Printing note: If you do not wish to print this page, then select "Pages from: first page # to: last page #" on the print dialog screen

ABSTRACT

BIOREMEDIATION OF 2-CHLOROPHENOL IN A LABORATORY SOIL COLUMN

by
Timothy A. Coon

In-situ bioremediation offers the prospect of rendering organic contaminants harmless without having to remove them from the subsurface. It involves the modification of environmental factors to stimulate the biodegradation of chemicals in the subsurface by microorganisms. However, for the cost-effective use of in-situ bioremediation, it is necessary to develop accurate engineering models to quantify biodegradation.

In this thesis, the biodegradation of 2-chlorophenol in a laboratory soil column was examined in order to experimentally verify an engineering model. Experiments were performed to obtain the physical and biological parameters required by the model, and the steady-state 2-chlorophenol distribution in the column.

A number of problems were encountered in obtaining consistent, reliable data. These problems were related to the use of a mixed microbial population, and the lack of significant adsorption on humic-free soil. A simplified version of the model indicated that most of the biomass was located in the lower (feed) end of the soil column.

BIOREMEDIATION OF 2-CHLOROPHENOL IN A LABORATORY SOIL COLUMN

by
Timothy A. Coon

A Thesis
Submitted to the Faculty of
New Jersey Institute of Technology
in Partial Fulfillment of the Requirements for the Degree of
Masters of Science

Department of Chemical Engineering,
Chemistry, and Environmental Science

January 1995

APPROVAL PAGE

BIOREMEDIATION OF 2-CHLOROPHENOL IN A LABORATORY SOIL COLUMN

Timothy A. Coon

Dr. Gordon Lewandowski, Thesis Advisor — Date
Chairperson and Professor of Chemical Engineering,
Chemistry, and Environmental Science, NJIT

Dr. Richard Trattner, Committee Member — Date
Associate Chairperson for Environmental Science
and Professor of Chemical Engineering, Chemistry,
and Environmental Science, NJIT

Dr. Piero M. Armenante, Committee Member — Date
Graduate Advisor for Chemical Engineering and
Professor of Chemical Engineering, Chemistry,
and Environmental Science, NJIT

BIOGRAPHICAL SKETCH

Author: Timothy A. Coon

Degree: Master of Science in Environmental Science

Date: January 1995

Undergraduate and Graduate Education:

- Master of Science in Environmental Science,
  New Jersey Institute of Technology,
  Newark, NJ, 1995

- Bachelor of Science in Civil Engineering,
  Massachusetts Institute of Technology,
  Cambridge, MA, 1987

Major: Environmental Science

ACKNOWLEDGMENT

I would like to express my sincere gratitude to my advisor, Dr. Gordon Lewandowski, for his guidance and support throughout this research. I am also thankful to Professors Richard Trattner and Piero M. Armenante for serving as members of my committee.

Special thanks to Dr. Sitaram Dikshitulu for his help and guidance during the experimental work and his continued assistance after he left NJIT to start a new job. I am also grateful to Kung-Wei Wang for his help and advice in Sitaram's absence.

Finally, I would like to thank my wife for her patience and understanding throughout this difficult experience.

TABLE OF CONTENTS

TABLE OF CONTENTS
(Continued)

Chapter **Page**

LIST OF TABLES

LIST OF FIGURES

LIST OF FIGURES
(Continued)

Figure **Page**

LIST OF FIGURES
(Continued)

Figure **Page**

LIST OF FIGURES
(Continued)

Figure **Page**

CHAPTER 1

INTRODUCTION

Significant quantities of organic pollutants have been released to the environment as a result of past waste disposal practices, leaking underground storage tanks, and accidental spills. These organic pollutants have migrated into the soil and ground water where they may persist for years, affecting water quality and limiting land use. Many organic pollutants are suspected human carcinogens or are toxic to humans and animals. Thus, there is an increasing concern regarding the fate and transport of organic chemicals in the subsurface, and a need to remove them in a cost effective manner.

Past solutions to the problem of contaminated soil in the United States involved excavation and disposal in landfills. Recently, however, the National Oil and Hazardous Substances Pollution Contingency Plan was amended to emphasize the use of permanent solutions and alternative treatment technologies that shift away from land disposal (EPA 2/91 and EPA 9/91).

Today's remediation technologies can be divided into ex-situ and in-situ methods. Ex-situ technologies (incineration, thermal desorption, soil washing, chemical extraction, etc.) require the excavation of the soil for treatment. Excavation and handling of soil, particularly at sites where there is a large volume of soil or where contamination extends well below the ground surface, can become very expensive. In addition, if ground water is contaminated at the site, it has to be dealt with separately. By contrast, in-situ technologies can be applied to the soil without disturbing it (thus avoiding solids handling costs), and can simultaneously treat the ground water.

Four of the most commonly used in-situ treatment technologies include solidification/stabilization, vacuum extraction, soil flushing, and bioremediation (EPA 9/91). However, not all of these can successfully treat organic contamination of the

subsurface and ground water. Solidification/stabilization involves mixing a chemical binder with the soil in place to immobilize the contaminants. This technology is normally applied to inorganic contaminants and may require pre-treatment of organics to be effective (Barth and Wiles 1989). Vacuum extraction involves moving air through the subsurface to increase chemical volatilization rates and treating the air stream. This technology is applicable to sites contaminated with volatile organics but is ineffective in the removal of nonvolatile organics. Similarly, soil flushing involves pumping ground water so that contaminants can dissolve and be pumped to the surface for treatment. However, hydrophobic contaminants can sorb strongly to soil making them difficult to remove completely, causing such soil flushing systems to be inefficient and slow. In addition, the processes frequently used to treat extracted water, air stripping and carbon adsorption, do not destroy contaminants but rather transfer them to another medium (Bouwer 1992).

In-situ bioremediation is one alternative that offers the prospect of rending organic contaminants harmless without having to remove them from the subsurface. Many organic compounds can be degraded by indigenous microorganisms (Hinchee and Olfenbuttel 1991). According to Bouwer (1992), the objective of in-situ bioremediation is to modify environmental factors, particularly concentrations of nutrients (nitrogen, phosphorous, etc.) and electron acceptors (oxygen, nitrogen, sulfate, etc.), to stimulate the biodegradation of chemicals in the subsurface by indigenous or introduced microorganisms. Ground water flow facilitates the transport of nutrients and electron acceptors necessary for the degradation of organic chemicals by microorganisms. Therefore, in-situ bioremediation is generally applicable to the saturated zone, which consists of packed soil particles with water moving through the pore spaces.

For the cost-effective use of in-situ bioremediation at contaminated sites, it is necessary to develop accurate engineering models to quantify biodegradation. Trial and error methods of implementing in-situ bioremediation at a site can be inefficient and

costly. Engineering models which combine physical, chemical, and biological processes in the subsurface can be used to identify potential problems, optimize the remediation process, and predict treatment time and costs. Major physiochemical and biochemical processes which can effect the concentration of organic contaminants in the ground water include dispersion, advection, diffusion, sorption, and biodegradation.

This research was performed to experimentally verify an engineering model developed by Dr. Gordon Lewandowski and Dr. Sitaram Dikshitulu at the New Jersey Institute of Technology. Their model incorporates two elements lacking in existing models: the growth of biomass coupled with non-equilibrium sorption/desorption processes. The in-situ bioremediation of the hydrophilic organic contaminant 2-chlorophenol (2CP) was simulated in a soil column seeded with a mixed microbial culture. Required model parameters were determined in the laboratory and used in the model to predict the distribution of 2CP as it underwent biodegradation in the soil column. Since a numerical solution to the model has yet to be obtained, a much simplified version was used for the data correlation.

CHAPTER 2

LITERATURE REVIEW

Two key processes which affect the persistence of organic chemicals in the subsurface are sorption and microbial degradation (McCarty *et al.* 1981, 1984). A large amount of research has been conducted to try to determine how these processes should be modeled to most accurately simulate the natural environment.

Sykes *et al.* (1982) developed one of the first engineering models for predicting the concentration of leachate organics, measured as chemical oxygen demand(COD), in the ground water below sanitary landfill sites. The model includes the processes of advection, dispersion, and simultaneous anaerobic substrate utilization and biomass production. Michaelis-Menten equations are used to describe substrate utilization and biomass production. The model was reduced to a first-order reaction kinetic model which was used to predict the COD distribution moving away from the landfill. The model appeared to over-estimate COD concentrations. The high predicted concentrations may have been due to the fact that the model ignored sorption processes.

Ogram *et al.* (1985) performed laboratory experiments to determine the effects of sorption on the biodegradation rates of (2,4-Dichlorophenoxy) acetic acid (2,4-D) in soils. The study showed that only 2,4-D in the solution was available for biodegradation and that sorbed 2,4-D was unavailable. The authors postulated that sorbed 2,4-D was either sufficiently deep within the soil matrix so that bacteria could not attack it or that bacteria were simply unable to take up 2,4-D from the sorbed phase. In either case, it was shown that sorption limited the availability of organic contaminants for biodegradation.

Borden and Bedient (1986) developed a model to describe aerobic biodegradation in the subsurface which accounted for sorption. Their set of equations describes the simultaneous growth, decay, and transport of microorganisms, as well as the transport

and removal of hydrocarbons and oxygen. The methodology differs from Sykes in that the model takes into account the mechanisms of adsorption and oxygen transport from the unsaturated zone. Borden and Bedient felt that adsorption could have an important influence on oxygen-limited biodegradation by allowing non-retarded oxygen to move into the slower moving contaminant plume. Adsorption is modeled as a linear instantaneous reaction and biomass growth is modeled using a modified Monod equation. The model also assumes that the microbes are attached to the soil. It was concluded that for oxygen limited biodegradation, consumption of oxygen and hydrocarbon can be approximated as an instantaneous reaction which simplifies the model. A field application of the model showed that simulated oxygen and hydrocarbon concentrations were close to the observed values (Borden *et al.* 1986).

Srinivasan and Mercer (1988) built on the work of Borden and Bedient. They developed a one dimensional (1-D) model for simulating biodegradation and sorption processes in saturated porous media. Their model uses equilibrium isotherms developed by Freundlich and Langmuir to account for the rapid surface adsorption phenomenon. However, the model ignores the slower time dependent phenomenon of diffusion into the soil matrix. The model is also simplified by assuming that the biomass concentration is constant. They justified this assumption using results from Borden *et al.* (1984) which showed that in field situations, microbial growth reaches equilibrium rapidly relative to ground water flow and large variations in microbial population and growth kinetics have little effect on contaminant distribution. They also referred to biofilm studies (Bakke 1986) that shows biofilm thickness reaches a maximum early and remains constant. Model simulations were shown to closely match the Borden and Bedient results. However, Srinivasan and Mercer concluded that the assumption of a constant biomass concentration was a major limitation of their model.

Semprini and McCarty (1991) developed a model similar to Borden and Bedient (1986) which includes advection, dispersion, microbial growth and substrate utilization,

and sorption. Microbial growth and substrate utilization is modeled using Monod kinetics. Sorption is modeled using equilibrium processes. The biomass is assumed to be fixed in a biofilm. However, the biofilm is assumed to be fully penetrated with substrate. This assumption simplifies the model since diffusion into the biofilm need not be considered. The model simulations were compared to the results of field experiments involving methane utilizing bacteria in a semiconfined aquifer. Simulations provided good correlation to the observed data demonstrating that the relatively simple model could be used in the design and evaluation of in-situ bioremediation processes. However, it was concluded that specific microbial parameters needed for the model were high and may have been the result of neglecting mass transfer effects across the biofilm. In addition, the chemical used in the experiments did not adsorb to the soil. Thus, the model effectiveness for hydrophobic contaminants could not be evaluated.

The three models discussed above use linear equilibrium relationships to describe sorption in their models. The linear equilibrium assumption, however, does not always provide an adequate description of organic contaminant sorption.

Robinson *et al.* (1990) performed batch soil microcosm experiments to evaluate the sorption and bioavailability of toluene in an organic soil. It was determined that the sorption of toluene occurs in two phases. There is an initial period of rapid sorption followed by continued sorption at a much slower rate until equilibrium is reached. This research suggests that sorption is a non-linear process. It was concluded that a small quantity of toluene desorbs very slowly, and biodegradation may be limited by the desorption rate.

Research by Bahr (1989) supports the concept of non-linear, desorption-rate-limited biodegradation. Bahr conducted field experiments at the Gloucester Landfill near Ottawa Canada where soil flushing was being performed as a treatment method. He found that at high pumping rates, where concentrations in the water were decreased, there

was still a significant mass of contaminant sorbed to the soil. He concluded that this was due to non-equilibrium desorption rates.

Pickens *et al.* (1981) provides further proof of the non-equilibrium nature of the adsorption/desorption phenomenon. Radial injection dual tracer studies were performed in a sandy aquifer to determine the dispersive and adsorptive properties. Nonlinear rate-limiting desorption was indicated by extreme tailing of tracer breakthrough curves.

Pignatello (1989) reviewed evidence for the various factors controlling sorption non-equilibrium. These factors include: 1) mass transport of organic compounds between the bulk liquid phase and the soil aggregate surface, 2) mass transport within the internal soil aggregate, and 3) the kinetic rate limitations of the surface reaction itself. A review of the literature by Scow and Hutson (1992) found increasing evidence supporting the view that the internal pore diffusion controls the overall sorption rates.

In order to simulate the complex processes that affect the sorption of organic chemicals, in particular internal pore diffusion, researchers began using two compartment models. Wu and Gschwend (1986) were one of the first to develop a spherical-aggregate model to describe diffusion-limited sorption of organic chemicals. The concept behind the model was that organic molecules must diffuse through the immobile pore fluids held in the interstices of natural soil aggregates, where penetration is retarded by microscale partitioning of molecules between sorbed and dissolved phases.

This concept was applied to modeling the movement of non degradable organic compounds in soil by Crittenden *et al.* (1986). They developed a two compartment model to describe the migration of non degradable, organic chemicals through a column of saturated aggregate soil. The model assumes that the soil is uniform, stationary, spherical aggregates composed of soil particles and stagnant water. Processes included in the model are transport and retardation mechanisms of advective flow, axial dispersion, liquid-phase mass transfer, diffusion into immobile liquid, and local adsorption equilibrium. A number of analytical solutions to the model based on a wide range of

simplifying assumptions were used to predict the 1-D concentration profile of a chemical flowing in the soil column. Comparing the predicted behavior to experimental soil column results, the researchers were able to evaluate their simplifying assumptions and assess the importance of various mechanisms. They concluded that few of the solutions were totally satisfactory because they did not account for all significant mechanisms. They found that non-linear adsorption, dispersion, liquid-phase mass transfer resistance, and diffusion into the stationary mobile phase all promote chemical spreading to some extent and cannot be completely ignored in any model.

Recent research has begun to apply the two compartment model concept to bioremediation of organic contaminants. Rijnaarts *et al.* (1990) performed laboratory experiments to determine the effect of desorption and intra-particle mass transfer on biodegradation of α-Hexachlorocychlohexane in suspended slurries of contaminated soil. They applied a first order model and a sorption-retarded radial diffusion model (a two compartment model) to the desorption and biodegradation kinetic data. Biomineralization was found to be limited by the desorption rate. The desorption rate was found to be limited by the intraparticle mass transfer. They found good correlation between the radial diffusion model which accounted for an intraparticle mass-transfer resistance as a function of the aggregate size. The first order model, though not as good as the radial diffusion model, also performed adequately.

Scow and Hutson (1992) studied the effect of chemical availability on biodegradation and developed a model using the two compartment concept to describe the experimental results. Major aspects of the model are 1) sorption of the chemical to the solids is described by a linear equilibrium isotherm, 2) biomass is assumed to be uniformly distributed in the solution outside of the aggregates only, and 3) biodegradation is simulated using Monod kinetics assuming no net growth in biomass. It was concluded that the two compartment model provided a better correlation than does the first order model where the chemical availability is limited by both diffusion and sorption.

However, a first order model is sufficient in cases when diffusion is less important (i.e. where aggregates have small radii or when there is a high ratio of solution outside to solution inside). One of the major limitations of the model was determined to be the assumption that bacteria were only present in the solution phase outside the aggregate when they are likely attached to the surfaces.

As discussed above, several engineering models have been developed for the biodegradation of organic contaminants in the subsurface. Some of the models incorporate biomass growth, but lack a complete description of non-equilibrium sorption processes. Others use two compartment models to describe non-equilibrium sorption, but fail to couple these processes with biomass growth. The present study focuses on validation of an engineering model developed by Lewandowski and Dikshitulu, which incorporates the dynamic interplay between sorption, biodegradation, and biomass growth.

CHAPTER 3

OBJECTIVE

The objective of the present study was to experimentally evaluate the engineering model of in-situ bioremediation proposed by Dr. Gordon Lewandowski and Dr. Sitaram Dikshitulu at the New Jersey Institute of Technology. A brief description of the model is presented in Chapter 4. The model incorporates biomass growth and non-equilibrium adsorption/desorption processes in the simulation of in-situ bioremediation in the saturated zone.

The objective was met in three steps. The first step was the performing laboratory experiments to determine the physical and biological parameters required by the model. The second step was measuring the biodegradation of 2-chlorophenol in a soil column, and determining the steady state contaminant distribution. The final step was using the model to correlate the distribution of 2-chlorophenol in the soil column, and comparing the model values to experimental results.

CHAPTER 4

MATHEMATICAL MODEL

The model proposed by Lewandowski and Dikshitulu of in-situ biodegradation in the saturated zone utilizes a two compartment concept that differs from previous models in two important ways:

1) coupling of non-equilibrium sorption to bioavailability, and
2) allowing for biomass growth,

both of which are very important to real in-situ situations.

The two regions of the model are the aggregate phase and the mobile phase. These regions are illustrated in Figure 1. The aggregate phase is conceptualized as spherical soil clumps which contain internal stagnant water. The mobile phase is composed of ground water flowing between the aggregates.

The resulting partial differential equations which are used to represent pollutant behavior in these phases are parabolic and non-linear. These equations are briefly described below. Equation parameters are defined in Table 1 at the end of this chapter.

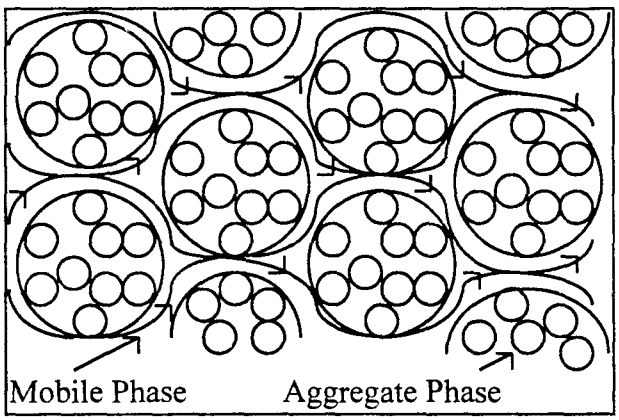

Figure 1 Illustration of two compartment model.

The change in pollutant concentration with respect to time within the spherical aggregates is represented by the following equation:

$$\frac{\partial C_a}{\partial t} = D_{se}\left\{\frac{1}{r^2}\frac{\partial}{\partial r}\left(r^2\frac{\partial C_a}{\partial r}\right)\right\} - B_d - A_d \tag{4.1}$$

The first term on the right in equation 4.1 represents diffusion of the pollutant into and out of the aggregate. The second term represents the biodegradation rate. The third term represents the sorption rate onto the solids. The third term can be positive or negative depending on whether the pollutant is adsorbing or desorbing.

The biodegradation term in equation 4.1 can be expressed as:

$$B_d = \frac{b}{Y}\left(\frac{\hat{\mu}C_a}{K_s + C_a + \frac{C_a^{\,2}}{K_i}}\right) \tag{4.2}$$

which is affected by biomass growth:

$$\frac{\partial b}{\partial t} = b\left(\frac{\hat{\mu}C_a}{K_s + C_a + \frac{C_a^{\,2}}{K_i}}\right) - \hat{\mu}_c \tag{4.3}$$

The term within the parenthesis in equations 4.2 and 4.3 is the specific growth rate for an inhibitory substrate as described by the Andrews' model.

The sorption term in equation 4.1 can be expressed as:

$$A_d = k_d\left(C_a - C_a^{\,*}\right) \tag{4.4}$$

This is related to sorption onto the solids by the equation:

$$\frac{\partial q}{\partial t} = \frac{\varepsilon_a}{\rho_s(1-\varepsilon_a)}\left\{k_d\left(C_a - C_a^{\,*}\right)\right\} \tag{4.5}$$

in which q is related to the equilibrium fluid-phase concentration (C_a*) by the Freundlich equation:

$$q = k_p\left(C_a^*\right)^{\frac{1}{n}} \tag{4.6}$$

Within the aggregate, the following initial and boundary conditions apply:

At t=0: $C_a=C_{ao}(r,z,0)$; $b=b_o(r,z,0)$; and $q=q_o(r,z,0)$.

At r=0: C_a is finite (i.e. $\frac{\partial C_a}{\partial r}=0$).

At r=R: $-D_{se}\frac{\partial C_a}{\partial r}=k_m\left(C_a-C_b\right)$.

Since $C_b=C_b(z,t)$, the equations must be solved at a given value of z.

The change in pollutant concentration with respect to time within the mobile phase is represented by the following equation:

$$\frac{\partial C_b}{\partial t}=D_{le}\frac{\partial^2 C_b}{\partial z^2}-\overline{V}_z\frac{\partial C_b}{\partial z}+\frac{(1-\varepsilon)}{\varepsilon}k_m\frac{3}{R}\left[C_a\big|_{r=R}-C_b\right] \tag{4.7}$$

The first two terms on the right in equation 4.7 represent the axial diffusion and axial convection of the pollutant, respectively. The third term represents the mass transfer of the pollutant from the aggregates to the mobile phase. The surface to volume ratio for the spherical aggregates is 3/R.

The applicable initial and boundary conditions for equation 4.7 are:

At t=0: $C_b=C_{bo}(z,0)$;

At z=0: $D_{le}\frac{\partial C_b}{\partial z}=\overline{V}_z C_b$; and

At z=L: $C_b=C_{bL}$ [or at $z=\infty$: $C_b=0$, or $\frac{\partial C_b}{\partial z}=0$]

Unfortunately, a complete solution to the model has yet to be developed. Therefore, for the purpose of this research, a simplified analytical solution for steady state conditions was developed. By substituting scaling factors (listed in Table 1) into the

model, several terms were assumed to be negligible. The scaling factors include order of magnitude estimates of parameters obtained from the literature and from this study.

Assuming that we start with clean soil and the kinetic term is linear, the above equations can be simplified to:

$$\frac{dC_b}{dt} = -V_z \frac{dC_b}{dz} - KC_b \tag{4.8}$$

where $KC_b=B_d+A_d$. At steady state, equation 4.8 simplifies to:

$$\frac{dC_b}{C_b} = -\frac{K}{V_z} dz \tag{4.9}$$

Integration of equation 4.9 yields:

$$\ln C_b = -\frac{Kz}{V_z} + k \tag{4.10}$$

For the condition that $C=C_{bo}$ at $z=0$, equation 4.10 becomes:

$$\ln\left(\frac{C_b}{C_{bo}}\right) = \left(\frac{-K}{V_z}\right) z \tag{4.11}$$

At small values of C_b, K can be estimated by:

$$K \approx \left[\frac{\hat{\mu} b}{K_s Y} + k_d\right] \tag{4.12}$$

Substituting equation 4.12 into equation 4.11 results in the following simplified steady state solution for small values of C_b:

$$\ln\left(\frac{C_b}{C_{bo}}\right) = -\left[\frac{1}{V_z}\left(\frac{\hat{\mu} b}{K_s Y} + k_d\right)\right] z \tag{4.13}$$

Equation 4.13 was used to correlate the steady-state 2-chlorophenol profile in the laboratory soil column.

Table 1 Definition of model parameters

Symbol	Parameter	Units	Scaling Factor
	Within Aggregates		
C_a	pollutant concentration	mg/l	
D_{se}	effective diffusivity	cm^2/sec	10^{-6}
r	radial distance	cm	
B_d	biodegradation rate	mg/l/sec	
A_d	adsorption rate	mg/l/sec	
$\mathbf{k_d}$	adsorption rate constant	sec^{-1}	0.0123
C_a^*	pollution concentration in liquid voids in equilibrium with solids	mg/l	
$\mathbf{k_p}$	Freundlich parameter	$(l/kg)^{1/n}$	19.6
n	Freundlich parameter		1
q	pollutant concentration on solid	mg/kg solid	
ρ_s	solid density	mg/l	1
ε_a	void fraction within the aggregate		0.19
R	aggregate radius	cm	0.1
b	biomass concentration	mg/l	
Y	yield coefficient	mg biomass /mg pollutant degraded	0.3
$\hat{\mu}$	Andrews' parameter	sec^{-1}	0.26
$\mathbf{K_s}$	Andrews' parameter	mg/l	35
$\mathbf{K_i}$	Andrews' parameter	$(mg/l)^{-1}$	13
μ_c	decay coefficient	sec^{-1}	0.1
k_m	mass transfer coefficient	cm/sec	
t	time	sec	
	Within Mobile Phase		
C_b	pollutant concentration	mg/l	
$\mathbf{D_{le}}$	axial diffusion coefficient	cm^2/sec	10^{-5}
ε	void fraction within the mobile phase		0.11
V_z	average water velocity	cm/sec	50
L	length of plume	cm	
z	axial distance	cm	

Note: Bold symbols denote input parameters which are experimentally determined in this study.

CHAPTER 5

MATERIALS AND EXPERIMENTAL PROCEDURES

5.1 Microorganisms and Medium

Approximately 5 liters of secondary treatment sewage sludge (mixed liquor) was obtained from the Passaic Valley Waste Water Treatment Facility as a source of microorganisms. A portion of the mixed liquor was acclimated to 2-chlorophenol (2CP) as described below.

A primary culture was prepared by transferring a loop of the mixed liquor into approximately 100 ml of defined medium in a 250 ml flask. 2CP stock solution was added to obtain a concentration of about 5 mg/l. The flask was stoppered with a cotton plug and placed in a New Brunswick Scientific Co., Inc. Series 25 Incubator Shaker at 200 rpm and 22°C. The medium was aerated by virtue of the shaking process only. The medium was sampled regularly and spiked with 2CP stock solution when necessary to obtain the desired concentration. The concentration was initially maintained between 5 and 10 mg/l and was increased as the culture continued to grow.

This procedure was repeated for a secondary and tertiary culture. The secondary and tertiary cultures were inoculated with microorganisms from the primary and secondary cultures, respectively. The growth of the secondary and tertiary cultures was erratic and inconsistent, however. The reason for the inconsistent growth could not be determined. Possible reasons could have been oxygen limitations, pH fluctuation, or competition between the microorganisms in the culture. Eventually these cultures were abandoned and a different acclimation process was employed.

Continued acclimation of the primary culture was performed in a batch reactor. The reactor consisted of a 5-liter Lucite cylindrical vessel capped with a removable lid and filled with approximately 2 liters of defined medium. Laboratory compressed air was

constantly bubbled through the reactor to provide excess oxygen. Air entered through a porous stone diffuser near the bottom of the reactor. A mechanical stirrer provided constant agitation.

The batch reactor was inoculated with a portion of the primary culture and spiked with 2CP stock solution to obtain a concentration of around 5 mg/l. The 2CP concentration and pH were monitored regularly. A 5% phosphate buffer solution (K_2HPO_4) was added to the medium when necessary to maintain the pH around 7.2. When the 2CP concentration reached zero in the reactor, more stock solution was added to achieve the desired concentration. Acclimation in the batch reactor started at concentrations of 5 to 10 mg/l and was increased with the growth and performance of the culture. This process ensured that the culture had fully adapted to growth on the 2CP medium, and that 2CP was the sole carbon source.

During this acclimation process, several samples of the acclimated culture were transferred from the reactor to agar plates (Bacto Nutrient Agar, Difco Laboratories) and nutrient broth (BBL®) in test tubes, incubated for a period of 24 to 48 hours, and then placed in the refrigerator at 4°C. These cultures were stored for later use during the kinetic experiments.

The composition of the defined medium used for the cultivation and maintenance of the microorganisms is shown in Table 2. The medium was prepared using tap water, and maintained a pH of 7.2.

5.2 Kinetics Determination

The acclimated microbial consortia was used in batch reactor experiments to determine the kinetics of the removal of 2CP. Two batch reactors were run simultaneously during the kinetic experiments. The reactors were set up the same as the reactor used for the acclimation of the culture with 2 liters of defined medium, constant bubbling of air, and mechanical agitation. All experiments were run at room temperature which

Table 2 Composition of defined medium

Component	Concentration (g/L)
K_2HPO_4	5.803
KH_2PO_4	2.268
$(NH_4)_2SO_4$	0.5
$MgSO_4$	0.1
$MnSO_4$	0.01

ranged from about 19°C to 26°C. The pH of the medium was measured prior to each individual kinetic experiment and adjusted to maintain a pH of about 7.2. Actual pH ranged from about 7.15 to 7.25 during all of the experiments. A buffer of 5% potassium phosphate solution (K_2HPO_4) was used to increase the pH when necessary.

The reactors were initially inoculated with acclimated culture obtained from storage in nutrient broth. Several kinetic experiments were then conducted using the same biomass at increasing initial concentrations. It was observed that when biomass concentrations reached a certain level (optical density of approximately 0.150), the biomass began to agglomerate and settle. This hampered optical density measurements. When this occurred, the reactor was emptied, cleaned, filled with fresh defined medium, and inoculated with either biomass in medium set aside before emptying the reactor, or from cultures maintained in nutrient broth in the refrigerator.

To begin a kinetic experiment, a small amount of 2CP was added to the reactor to activate the culture. After about 15 to 20 minutes, a larger slug of stock 2CP solution was added to obtain the desired initial concentration. The medium was given a few minutes to mix and was then sampled. The medium was sampled initially and at 30 minute to 1

hour intervals. Each sample was analyzed for biomass concentration and for substrate (2CP) concentration. Results for each kinetic run are presented in Table A-1 through A-11 in App. A.

5.3 Confirmation of Microbial Degradation

The release of chloride during batch reactor experiments was used as an indicator that 2CP removal was a result of microbial degradation. These experiments were run similar to the kinetic experiments described above. However, de-ionized water was used to prepare the defined medium instead of tap water to reduce the background chloride concentration. Iron was added to the medium at a concentration of 0.5 mg/l to replace trace iron initially supplied by tap water. 2CP stock solution was added to the inoculated medium to obtain the desired concentration, and the initial concentration was measured. The chloride concentration was measured prior to the addition of 2CP and again when the 2CP concentration had decreased to zero using a calibrated chloride specific ion electrode as described below.

5.4 Soil Characteristics

5.4.1 Composition

An uncontaminated composite soil was prepared for this study using 10% (by volume) clay, 40% fine sand, and 50% silty sand. The clay was 100% kaolinite. The fine sand was a silica sand (30-100 mesh) from MacMaster-Carr Supply Company in New Brunswick, New Jersey. The silty sand was obtained by passing material obtained from a sand and gravel pit in Mahwah, New Jersey, through a No. 25 mesh sieve (56% of the original material passed through a 200 mesh screen).

Initially a soil composite of 60% silty sand and 40% fine sand was used. Since a negligible amount of 2CP was adsorbed to that mixture, clay was substituted for 10% of the silty sand. Although some adsorption was then observed (see Results and

Discussion), that may have been an artifact, and adsorption may be principally determined by the amount of natural organic material (humic substances) present in a native soil (but neglected in this study).

The composition of sand, silt, and clay was consistent with water percolation rates on the order of 10 cm/hour, which was an experimental objective based on "typical" ground water flow velocities. A higher sand content resulted in higher percolation rates, while a higher silt and clay content resulted in lower percolation rates.

Table 3 compares the soil used in this study with United States Environmental Protection Agency (USEPA) standard soils and Eurosoils.

Table 3 Comparison of test soils

	This Study	USEPA "Standard" Soil*	Eurosoil No. 3**
Gravel	-	3%	-
Sand	40%	56%	46
Silt	50%	29%	36
Clay	10%	12%	17
Organic Material	-	3.2%	3.7
pH	8.1	8.5	5.3

* The clay used in the USEPA study was 70% kaolinite and 30% bentonite or montmorillinite. Information obtained from Esposito, *et al.*, 1989.

** Information obtained from Kuhnt, 1990.

In addition, a #2 widely graded, coarse sand, 8-16 mesh (The Morie Company, Moses, Indiana), was used around the sampling ports to prevent clogging of the sampling needle.

5.4.2 Total Porosity

The total porosity of the composite soil and the coarse sand used in packing the column was determined. A sample of soil was placed in a test tube and the tube was tapped slightly to compact the soil. The level of the top of the soil was marked on the tube to

denote the total volume. The mass of the test tube and soil was measured. Water was added and allowed to fully saturate the soil. Excess water was removed with a medicine dropper. The mass of the test tube, soil, and water was measured. The mass of the test tube and soil was subtracted from the mass of the test tube, soil, and water to determine the mass of water added. This value was divided by the density of water (1 g/ml) to determine the volume of water in the saturated soil matrix.

The soil and water were then removed from the test tube and the tube was cleaned and dried. The empty, dry tube was then weighed. Water was added to the mark on the tube denoting the total volume the soil had occupied, and the tube weighed again. The mass of the empty tube was then subtracted from the mass of the tube plus the water to determine the mass of water occupying the same total volume as the soil matrix. This value was divided by the density of water (1 g/ml) to give the total volume of the soil matrix.

The volume of the water in the soil matrix, divided by the total volume of the matrix, equals the overall porosity of the soil. This procedure was performed twice, with both the composite soil and the coarse sand. The average total porosity of the composite soil was 27.5% and the average total porosity of the coarse sand was 44.5%. Based on the composition of the packed column (Figure A-1 in App. A), the average porosity of the column was

5.4.3 Internal Aggregate Porosity

The porosity within the "aggregates" of the composite soil was estimated by adding water to a given volume of soil in a manner such that the pore spaces remained open, but the aggregates absorbed the water. A small portion of soil was placed in a burette and the total volume occupied by the soil (including void space) was recorded. Water was added to the soil in 0.2 ml increments to allow the water to travel down the soil column by gravity, saturating the aggregates but leaving larger pore spaces open. The wetted

volume resulting from each 0.2 ml increment of water could be observed visually in the burette and was recorded. Dividing 0.2 ml of water by the wetted volume (observed in ml) was taken as an indication of the fraction of the total volume occupied by voids within the aggregates for that increment. The incremental percentages were averaged over the entire length of the soil in the burette. This procedure was performed twice for confirmation. The final estimate for the percentage of the total volume occupied by aggregate voids was 16.7%.

5.5 Batch Adsorption Experiments

Batch experiments were performed to determine the rate of adsorption of 2CP by the composite soil. Initially, a 15 g sample of the composite soil was placed in a 250 ml flask with 100 ml of 2CP solution at an initial concentration of 7.16 mg/l. A control flask containing 100 ml of 2CP solution with no soil added was also prepared. The two flasks were placed in the incubator shaker at 22°C and 200 rpm. Liquid samples were collected periodically and assayed to determine how much 2CP was removed from the water by the soil. Sampling continued until the 2CP concentration of the liquid stabilized (i.e. no longer decreased). At this point, 2CP was considered to be in equilibrium between the soil and the water phases.

Subsequent batch experiments were performed to confirm the results of the initial experiment. Three soil samples of different size (15, 22.5, and 30 g) were mixed in 250 ml flasks with 100 ml of 2CP solution at an initial concentration of 6.2 mg/l. It was necessary to autoclave these soil samples at 101°C for 2 hours prior to adding the 100 ml of solution because the soil composite stock had become contaminated with microorganisms while in the lab. The flasks were placed in the incubator shaker at 22°C and 200 rpm and sampled periodically for 2CP. The results of the batch adsorption experiments are presented in Table A-12 in App. A.

5.6 Continuous Flow Soil Column

5.6.1 Column Configuration

The two columns used were glass manifolds with side ports (Ace Glass, Vineland, New Jersey). Their dimensions were 24 cm in height by 5 cm inside diameter with sampling ports at 2, 7, 12, 17, and 22 cm. Details of the column packing are shown in Figure A-1 in App. A. Columns were packed identically. A thin layer of glass beads (2 mm dia.) was placed on a plastic mesh at the bottom of the column to prevent fine particles from clogging the inflow tubing. Approximately 2.0 cm layers of coarse sand were packed around the sampling ports to prevent the finer particles of the composite soil from clogging the needle during sampling. The remainder of the column was filled with the composite soil. The column was wrapped in aluminum foil to prevent the growth of photosynthetic microorganisms.

Columns were packed with water present in the column to prevent air from being trapped in the soil matrix. Prior attempts to pack a dry column resulted in many air pockets which affected the dispersivity and porosity of the soil and the overall performance of the column.

Columns were arranged for column experiments as in Figure A-2 in App. A. A Cole Parmer, Masterflex® Model 7519-10, 6 Cartridge Pump with Digital Console Drive was used to pump the feed solution from a 20 liter feed tank through the packed column in an up-flow mode. The tubing consisted of Masterflex® 6426-16 tubing. A smaller tubing (Masterflex® 6426-13) was used initially but tended to slip through the pump at the required flow rates. Effluent was collected in a 20 L container.

5.6.2 Soil Column Tracer Studies

Chloride tracer experiments were performed in the packed columns to determine the dispersion coefficient of the soil. Sodium chloride (NaCl) was used as a conservative tracer. Distilled water was placed in the feed tank and pumped through the column at a

constant rate. Distilled water was used to minimize the background chloride concentration. At time zero, a slug (0.2 ml) of stock NaCl solution at a concentration of 1000 mg/l was injected into port 1. Samples were collected from port 5 periodically using a syringe equipped with a 2" stainless steel hypodermic needle. A sample size of 2cc was used to provide enough liquid to facilitate the use of the chloride meter. Samples were transferred to clean glass jars and analyzed for chloride. Experiments were run at 3 different flow rates: 0.85 ml/min, 1.05 ml/min, and 4.45 ml/min. Results are presented in Table A-13 in App. A.

5.6.3 Continuous Feed Column Studies

To initially seed the column, a 2CP degrading culture were first grown in a batch reactor as described above. The batch reactor was then used as a feed tank, and the contents were pumped through the column. The 2CP concentration in the reactor during the column seeding was maintained at 5 - 20 mg/l to keep the culture active. OD measurements of the effluent during the seeding stage indicated that the microorganisms were retained inside the column. The seeding proceeded at a flow rate of 0.85 to 1.5 ml/min.

Continuous feed studies proceeded by pumping a feed solution through the column at a constant flow rate and monitoring the concentration of the 2CP within the column over time. The feed solution was composed of defined medium spiked with stock 2CP solution to maintain the desired concentration of about 6 mg/l. Samples were collected periodically from sampling ports and analyzed for 2CP. Flow rates were also measured periodically. Results are presented in Table A-14 and Table A-15 in App. A.

During initial trials, the 2CP concentration was maintained around 16 mg/l and a flow rate of around 1 ml/min was used. However, under these conditions degradation was only occurring near the inlet to the soil column. It was proposed that this was due to an oxygen limitation. A calculation of the stoichiometric requirement of oxygen (MW = 32 g/mole) for the degradation of 2CP (MW = 128.56 g/mole) was performed.

$$2\ C_6H_5ClO + 13.5\ O_2 \rightarrow 12\ CO_2 + 5\ H_2O + 2\ Cl \qquad (5.1)$$

From the balanced equation 5.1, it was determined that the mass ratio of 2CP to oxygen is 1 : 1.68. If we assume that the medium was saturated with oxygen (8.0 mg/l), there was only enough oxygen present to degrade 4.76 mg/l of 2CP.

Therefore, an oxygen limitation existed at a feed concentration of 16 mg 2CP/l. As a result, the feed concentration was reduced to 6 mg 2CP/l. In addition, the flow rate was increased so that a 2CP profile could be measured further up the column. Trial and error was used to determine a flow rate (about 4.5 ml/min) that would allow for a distribution of the 2CP degradation over the entire column.

Another problem that arose during the continuos flow column studies was the contamination of the feed tank by microorganisms. This resulted in a decrease in the 2CP concentration in the feed solution. Several steps were taken in an attempt to remedy this. First, cotton was used to cover the top of the feed tank to prevent airborne microorganisms from contaminating the feed. Second, compressed air for aeration was passed through a biofilter prior to entering the feed tank. Third, fresh feed solution was prepared more frequently. Finally, air lines, air diffusers, and tubing which came into contact with the feed solution were cleaned with successive rinses of methanol and de-ionized water during feed tank changes. Despite these efforts, the actual 2CP feed concentration still decreased slightly.

5.7 Analytical Procedures

5.7.1 2-Chlorophenol Analysis

Liquid samples for 2CP analysis were collected using B-D® 3cc disposable syringes. Samples were prepared for analysis by passing them through 0.2 μm nylon membrane filters (Gelman Sciences). One drop of 6M HCl was added to acidify samples and insure that 2CP did not disassociate prior to analysis, resulting in values below the true

concentration. Samples were usually analyzed within one hour of collection. Samples not immediately analyzed were stored frozen.

2CP was measured using a Spectra Physics HPLC equipped with a SP8880 Autosampler, a Spectra 200 Programmable Wavelength Detector, a SP8800 Ternary HPLC Pump, and a SP850 Dynamic Mixer. The mobile phase consisted of A (1% acetic acid in methanol) and B (Millipore water). The ratio of A : B was 55 : 45, run isocratically. The flow rate was 1 ml/min. The column was a Merck 50829 LiChroshper ® 60 RP-select B (5 μm). The detector was set at 280 nm, 0.5 AUFS. The data was processed by PE Nelson Model 2600 Chromatography Software, rev. 5.10, interfaced with the PE Nelson 900 Series Interface. Under these conditions the retention time of 2CP was approximately 3.55 minutes. However, it fluctuated between 3.35 and 3.85 minutes depending on the room temperature.

Calibration curves for 2CP were prepared periodically throughout the course of the experiments by preparing and assaying solutions of known 2CP concentration. A minimum of 5 standard points was used for each calibration curve. The calibration curves were entered into the HPLC software so that it automatically determined 2CP concentrations during subsequent analyses. A typical calibration curve is shown in Figure A-3 in App. A. Standard samples were also run periodically to check the calibration curve. 2CP standard and stock solutions were prepared using SIGMA Chemical Co. 2-chlorophenol.

A set of duplicate standard samples was prepared to determine the accuracy and precision of the analytical method. Results were within ±5% of the actual concentration. The detection limit of the method was around 0.1 mg/l.

5.7.2 Biomass Analysis

The growth of the microorganisms was determined by measuring the optical density (OD) of a sample using a Varion DMS 200 UV-VISIBLE Spectrophotometer set at 540 nm.

OD was measured prior to filtering samples. A previous study by Dikshitulu (1991) determined that for pure phenol degrading cultures with OD less than 0.6 there is a linear relationship between optical density and biomass concentration with a slope of 273 g/m^3 (or mg/l) per unit optical density. For this study, it was assumed that size and light adsorption of the microorganisms of the 2CP degrading mixed culture was the same as the microorganisms of the pure phenol degrading culture. Thus, the same linear relationship of 273 g/m^3 biomass per unit optical density was used. All OD measurements were well below the linear limit of 0.6.

5.7.3 Chloride Analysis

Chloride concentrations were measured using an ORION Model SA 720 Chloride Meter with the ORION Model 96-17B Combination Chloride Electrode. The meter read out for each sample was given in millivolts. The chloride concentration was then calculated using a calibration curve of chloride concentration versus millivolts which was prepared according to the procedures described in the chloride meter manual. A typical calibration curve is shown in Figure A-4 in App. A.

The meter detection limit is specified as 1.8 mg/l. However, it was possible to obtain consistent chloride measurements as low as 0.6 mg/l with little scatter.

The calibration curve was prepared using a set of standard solutions with chloride concentrations ranging between 1 and 10 mg/l. Other standard samples with concentration of 0.5, 1.5, and 5.0 mg/l were then prepared to test the calibration curve. The resulting concentrations determined from the calibration curve were 0.80, 1.49, and 5.07 mg/l, respectively. This shows that the calibration curve is a little skewed giving over estimations at low concentrations and under estimates at high concentrations. This is to be expected because the validity of the linear relationship between millivolts and concentration is lost at low concentrations. However, the calibration curve is most accurate around the range measured in the experiments.

5.7.4 pH Measurement

pH was measured using an ORION Model EA920 Expandable ionAnalyzer with Model 91-56 combination pH electrode. The meter was calibrated periodically using pH = 4.04 and pH = 7 buffer solutions.

5.7.5 Flow Rate Measurement

The flow rate of the solution passing through the soil column was periodically measured by collecting the effluent in a graduated cylinder over a given period of time. The accuracy of this method was ±0.1 ml/min.

CHAPTER 6

RESULTS AND DISCUSSION

6.1 Andrews' Model Parameters from Batch Kinetic Experiments

Determination of the three Andrews' parameters and the yield coefficient were made in batch kinetic experiments using a mixed microbial culture.

The kinetic experiments produced data of biomass growth versus time and substrate utilization versus biomass growth for 11 initial substrate concentrations. The results for each kinetic run are presented in Tables A-1 through A-11 in App. A.

Plots of the natural log of the biomass concentration versus time (Figures A-5 through A-15 in App. A) were used to determine the slope of the exponential growth phase for each initial 2CP concentration. The slope of these curves, calculated using linear regression, yielded the specific growth rate. The calculated specific growth rates for each run are presented in Figures A-5 through A-15. Because the relationship between time and the natural log of the biomass becomes non-linear as it exits the exponential growth phase, only the linear portion of the curves were used in the calculation of the specific growth rates. In addition, specific data points which appeared to be in error were omitted from the calculation.

The yield coefficients for each run were determined by plotting the biomass concentration versus the 2CP concentration (Figures A-16 through A-26 in App. A). The slope of the line, determined by linear regression, is equal to the yield coefficient. All data points were used to obtain the yield coefficient. Calculated yield coefficients are presented on Figures A-16 through A-26. The yield coefficients ranged between 0.087 and 0.617 mg biomass/mg 2CP degraded. The average yield coefficient is 0.299 mg biomass/mg 2CP.

The Andrews' parameters $\hat{\mu}$, K_S, and K_i were determined using the calculated specific growth rates and the average 2CP concentrations during the exponential growth phase. Figure A-27 in App. A shows a plot of the calculated specific growth rates versus the average 2CP concentration. The curve is non-linear and implies substrate inhibition at high concentrations. This can be represented by the Andrews' expression:

$$\mu = \frac{\hat{\mu} C_a}{K_s + C_a + \frac{C_a^2}{K_i}} \tag{6.1}$$

where C_a is the 2CP concentration and μ is the specific growth rate. An attempt at using a non-linear regression computer program to fit the data to this expression proved futile due to the large amount of scatter and lack of data at low concentrations. Data at low concentrations could not be determined because the small increases in biomass at low concentrations could not be detected accurately using the optical density method.

A further attempt at determining the Andrews' parameters followed a methodology discussed by Shuler and Kargi (1992). This method assumes that at low concentrations, $C_a^2/K_i << 1$, and the inhibition effect is negligible. This reduces the Andrews' model to:

$$\mu = \frac{\hat{\mu}}{1 + \frac{K_s}{\hat{\mu}}} \quad \text{or} \quad \frac{1}{\mu} = \frac{1}{\hat{\mu}} + \frac{K_s}{\hat{\mu}} C_a \tag{6.2}$$

A plot of 1/u versus $1/C_a$ results in a line of slope $K_s/\hat{\mu}$ and intercept of $1/\hat{\mu}$. This curve was plotted in Figure A-28 in App. A. The resulting K_s and $\hat{\mu}$ are 18 mg/l and 0.13 sec^{-1}, respectively.

To solve for K_i, Shuler and Kargi assume that at high concentrations, $K_s/C_a << 1$, and inhibition is dominant. In this case, equation 6.1 reduces to:

$$\mu = \frac{\hat{\mu}}{1+\frac{C_a}{K_i}} \text{ or } \frac{1}{\mu} = \frac{1}{\hat{\mu}} + \frac{C_a}{K_i\hat{\mu}} \tag{6.3}$$

A plot of 1/u versus C_a at high concentrations results in a line of slope $1/(K_i*\hat{\mu})$ and intercept of $1/\hat{\mu}$. The resulting curve is shown in Figure A-29 in App. A. The best fit line at high concentrations results in negative values for K_i and u'. In addition, there was not agreement in the u' values determined by each curve. The negative parameters may have been due to the fact that the experimental concentrations were not very high and the condition $K_s/C_a << 1$ may not apply.

Therefore, as a third method, the K_s and $\hat{\mu}$ obtained from the approximation at low concentrations (K_s = 18 mg/l and $\hat{\mu}$ = 0.13 sec^{-1}) were used as a starting point for a systematic trial-and-error search of Andrews' parameters which reasonably fit the data. To initiate the search, the average concentration at which the peak growth rate occurred (C_{max}) was estimated from the data and Figure A-27. The initial estimate was 20 mg/l. Then using the following condition from Shuler and Kargi:

$$C_{max} = \sqrt{K_s K_i} \tag{6.4}$$

and the starting value of K_s (18 mg/l), a starting value of K_i was calculated. The three starting values for the three Andrews' parameters were then perturbed individually. After each perturbation, the new values of $\hat{\mu}$, K_s, and K_i were used to obtain three points on the curve (at S = 10, S = S_{max}, and S = 60 mg/l). These were plotted and compared to the experimental data. For all perturbations, the condition of equation 6.4 for K_s and K_i was maintained. This process was continued until a curve which reasonably fit the data was found. The resulting values of $\hat{\mu}$, K_s, and K_i which appear to fit the experimental data best are 0.26 sec^{-1}, 35 mg/l, and 13 mg/l, respectively. Figures A-30 through A-32 in App. A show the resulting curve compared to the experimental data and the results from slightly increasing and decreasing the estimated parameters. These figures demonstrate

that the chosen values best represent the data. However, 10% changes of these values do not appear to alter the correlation of the curve to the data significantly. In either case, the correlation between the curves and the data are not very good. However, we had to accept these estimates as the best that could be determined from the scattered data.

The large amount of scatter in the data and resulting poor fit to the Andrews' model may have been the result of many factors. It is believed that one of the main contributing factors was use of a mixed microbial consortium rather than a pure culture. The microorganisms in the mixed culture may respond differently to pH, temperature, and 2CP concentration, and the population may shift, producing scattered results.

As discussed in chapter 5, section 5.2, two batch experiments were performed to determine whether the removal of 2CP was the result of microbial degradation. The increase in chloride ion in the medium during 2CP removal was measured to indicate the release of chloride resulting from biodegradation of 2CP. Based on the balanced stoichiometric equation for the breakdown of 2CP (equation 5.1), 1 mole of chloride should be released for every mole of 2CP degraded. The initial 2CP concentrations of the two experiments were 14.37 and 14.07 mg/l. Using the ratio of the molecular weights of 2CP (MW=128.56) and chloride (MW=35.5) and the 1:1 molar relationship, the expected increase in chloride concentration in the medium for the two initial 2CP concentrations were 3.91 and 3.83 mg/l, respectively. The actual measured increases in chloride concentration were 4.4 and 5.51 mg/l, which is a recovery of 112% and 144%, respectively. The elevated recoveries may have been the result of the inaccuracies of the chloride meter measuring low initial chloride concentrations. In any case, it is apparent that chloride is released during the batch experiments. It was concluded that the removal of 2CP is largely the result of microbial degradation.

6.2 Void Fraction Parameters

According to Domenico and Schwartz (1990), typical total porosity values for fine sand and coarse sand range between 26 - 53% and 31 - 46%, respectively. The total porosity of a silty fine sand with clay would be expected to be in the lower range of the fine sands due to the presence of smaller silt and clay particles in the voids between the sand grains. The total porosity of the composite soil was estimated to be 27.5% which is in the expected range. In addition, the total porosity of the coarse sand was determined to be 44.5%, which also falls within the expected range.

To determine the void fraction within the mobile phase, ε, and the void fraction within the aggregate phase, ε_a, from the measured porosities, a 100 ml volume sample of composite soil was assumed. Based on the total porosity of 27.5%, the total volume of the voids in the assumed sample is 27.5 ml and the total volume of soil is 72.5 ml. From the experiments it was estimated that 16.7% of the total volume was occupied by voids within the aggregates. Thus, for the 100 ml sample, the void volume within the aggregates is 16.7 ml. The void volume outside of the aggregates is simply the difference between the total void volume (27.5 ml) and the void volume within the aggregates (16.7 ml) or 10.8 ml. Likewise, the total volume of the aggregates is equal to the void volume within the aggregate (16.7 ml) plus the volume of the soil (72.5 ml) or 89.2 ml. The void fraction within the mobile phase, ε, is equal to the void volume outside of the aggregates (10.8 ml) divided by the total volume (100 ml) or 0.108. The void fraction within the aggregate, ε_a, is equal to the volume of voids within the aggregate (16.7 ml) divided by the total volume of the aggregates (89.2 ml) or 0.187. These values, however, are counter intuitive. One would have expected the mobile phase void fraction (ε) to be greater than that of the aggregates (ε_a).

6.3 Adsorption Coefficients from Batch Adsorption Experiments

An estimate of the rate of adsorption of 2CP by the composite soil was determined from the initial batch adsorption experiment. The results of this experiment are presented in Table A-12 in App. A. Figure A-33 in App. A shows the remaining 2CP concentration in solution as a function of time. Based on the data, it appears that equilibrium is reached after approximately 300 hrs, and the liquid phase concentration at equilibrium, C*, is equal to 1.82 mg/l.

The equilibrium liquid phase concentration was used to determine the adsorption rate constant (k_d) using the following relationship:

$$\frac{dC}{dt} = -k_d(C - C^*) \tag{6.5}$$

where dC/dt is the rate of change in concentration over time. Integration of equation 6.5 yields:

$$\ln(C - C^*) = -k_d t + k' \tag{6.6}$$

which is a linear relationship. The constants k_d and k' in equation 6.6, are determined by plotting $\ln(C - C^*)$ versus time. The slope of the best fit line in the area where the curve is linear is equal to k_d, and the intercept is equal to k'. This plot is shown in Figure A-34 in App. A. The resulting k_d and k' are 0.01227 hr^{-1} and 1.794, respectively.

Another necessary adsorption rate constant for the model is the equilibrium rate constants of the Freundlich isotherm. The Freundlich isotherm relates the solid phase concentration, q, with the liquid phase concentration at equilibrium (C*). The equation is expressed as:

$$q = k_p(C^*)^{\frac{1}{n}} \tag{6.7}$$

It was assumed that the relationship in equation 6.7 is linear, with n equal to 1. This allows equation 6.7 to be reduced to:

$$k_p = \frac{q}{C^*} \tag{6.8}$$

The solid phase concentration can be calculated from the equilibrium liquid phase concentration as follows:

$$q = \frac{(C_{initial} - C^*)(V_l)}{M_s} \tag{6.9}$$

where $C_{initial}$ and C^* are in units of mg/l, V_l is the liquid sample size in liters, and M_s is the mass of the soil sample in kilograms. For the initial trial, 15 g of soil in 100 ml of solution at an initial concentration of 7.16 mg/l, with C^* equal to 1.82 mg/l, q is equal to 35.6 mg of 2CP/kg of soil. Substituting this value into equation 6.8, k_p is calculated to be 19.6 liters of solvent/kg of soil.

To confirm that these values were accurate, a second set of batch adsorption experiments were run using different amounts of soil (15, 22.5, and 30 g) in 100 ml of solution. The results of these experiments are presented in Table A-12 and shown in Figure A-35 in App. A. The liquid concentration in these experiments unexpectedly and suddenly went to zero after about 100 hours. It is believed that this was the result of contamination of the experiments with 2CP degrading microorganism. It is assumed that the data is acceptable up to 99.5 hours just prior to going to zero.

The values for k_p, k', and k_d estimated from the initial experiment were used to predict the adsorption behavior of the second batch of experiments. The predicted behavior was then compared to the experimental results to evaluate the accuracy of the estimated k_p and k_d. Combining equations 6.8 and 6.9 yields:

$$k_p = \frac{(C_{initial} - C^*)(0.1)}{(M_s)(C^*)} \tag{6.10}$$

Rearranging equation 6.10 to solve for C^* gives:

$$C^* = \frac{0.1C_{initial}}{k_p M_s + 0.1} \tag{6.11}$$

Solving equation 6.11 using the initial 2CP concentration of 6.2 mg/l, the masses of each of the samples, and the estimated k_p of 19.6 liters solvent/kg soil, gives predicted equilibrium concentrations of 1.57, 1.15, and 0.90 mg/l of 2CP for the 15, 22.5, and 30 g samples, respectively.

The predicted values of C^* for the second batch of experiments and the estimated values of k' and k_d from the initial experiment were then used to predict the liquid phase concentration at given times for the second round of experiments. Equation 6.5 can be rearranged as follows to solve for the concentration at a given time:

$$C = \exp(-k_d t + k') + C^* \tag{6.12}$$

Plugging in estimated values of k_d and k' yields:

$$C = 6.012\exp(-0.01227t) + C^* \tag{6.13}$$

Equation 6.13 was used to predict concentrations at given times for each of the secondary experiments. The predicted values are compared to the experimentally determined values in Table A-12 in App. A. There appears to be fairly reasonable correlation between the predicted data and the experimental data. Therefore, the estimated values of k_d and k_p and the assumption that n = 1 in equation 6.7 appear reasonable.

6.4 Dispersion Coefficient from Tracer Studies

Chloride tracer studies were run in the columns at three different flow rates (0.85, 1.05, and 4.45 ml/min) in order to determine the axial dispersion coefficient of the composite soil. The results of these experiments are presented in Table A-13 and shown in Figures A-36 through A-38 in App. A. During experiments at flow rates 0.85 and 1.05 ml/min, data were not collected at the tail end of the experiments. Therefore, a second order extrapolation was used to estimate the chloride concentrations at the end of these trials to compensate for the lack of data. For flow rate 0.85 ml/min, the data at times 145 - 195 minutes were used to extrapolate the data points at times 220 - 295 minutes. For flow

rate 1.05 ml/min, the data points at times 195 - 290 minutes were used to extrapolate the data points at times 315 - 365 minutes. Three separate experiments were run at flow rate 4.45 ml/min, and the average values were used for the estimation of the axial dispersion coefficient.

Following procedures described by Levenspiel (1972), an axial dispersion coefficient (D_{le}) was estimated for each flow rate using the mean and variance of the distributions shown in Figures A-36 through A-38 in App. A. The mean of the distribution curves represents the mean residence time of the chloride between the point of injection and the point of sampling (20 cm). The mean of the distribution is determined from discreet data using the following equation:

$$\bar{t} = \frac{\sum t_i C_i \Delta t_i}{\sum C_i \Delta t_i} \tag{6.14}$$

Likewise, the variance is given by:

$$\sigma^2 = \frac{\sum t_i^2 C_i \Delta t_i}{\sum C_i \Delta t_i} - \bar{t}^2 \tag{6.15}$$

The mean residence times and variances of the distributions for the three flow rates are shown on Figures A-36 through A-38.

The calculated mean residence time for the flow rate of 1.05 ml/min was unexpectedly larger than the mean residence time for the flow rate of 0.85 ml/min. This is likely attributable to the different columns used for the two experiments. Despite the fact that every effort was made to pack the columns identically, there was no way to control the final density and pore volumes of the columns. Thus, some variation in the column behavior was inevitable. The relative difference between the flow rates and residence times of these two experiments are not significant and do not appear to have a significant effect on the calculated dispersion coefficients.

As a check, the total porosities of the composite soil and the coarse sand was used to predict the residence time for each flow rate between port 1 and port 5. The total volume of the column between ports 1 and 5 is 393 cm^3. Based on the column packing configuration (Figure A-1 in App. A), this total volume is occupied by 265 cm^3 of composite soil and 128 cm^3 of coarse sand. Using the estimated porosities of the composite soil (27.5%) and the coarse sand (44.5%), the void volume between ports 1 and 5 is calculated to be 130 cm^3 (or 130 ml). The residence time is calculated by dividing the void volume by the flow rate. Thus, the predicted residence times between ports 1 and 5 at flow rates of 0.85, 1.05, and 4.45 ml/min are 153, 124, and 29 min, respectively. These are fairly close to the residence times obtained from the distribution curves.

For a closed vessel the variance of the distribution relates to the axial dispersion coefficient in the following manner:

$$\sigma_\theta^2 = 2\frac{D_{le}}{uL} \tag{6.16}$$

where σ_θ^2 is the dimensionless variance, u is the linear velocity of the chloride solution, and L is the distance that the chloride traveled. The dimensionless variance is related to the actual variance by:

$$\sigma_\theta^2 = \frac{\sigma^2}{\bar{t}^2} \tag{6.17}$$

Substitution and rearrangement of equations 6.16 and 6.17 yields:

$$D_{le} = \frac{\sigma^2 uL}{2\bar{t}^2} \tag{6.18}$$

Knowing that the velocity (u) is equal to the distance traveled (L) divided by the time of travel ($\bar{t}$), equation 6.18 becomes:

$$D_{le} = \frac{\sigma^2 L^2}{2\bar{t}^3} \tag{6.19}$$

Using L=20 cm and the means and variances for each tracer study (converted to seconds), equation 6.19 yields the axial dispersion coefficients of 2.31 $x10^{-3}$, 2.69 $x10^{-3}$, and 8.74 $x10^{-3}$ cm^2/sec for the flow rates 0.85, 1.05, and 4.45 ml/min, respectively. The average axial dispersion coefficient is 4.48 $x10^{-3}$ cm^2/sec. This is unexpectedly much larger than the molecular diffusion of about 10^{-6} cm^2/sec for organics in water.

6.5 Results of Continuous Flow Soil Column Experiments

Two sets of data were collected as a result of having to reseed the column during the experiment. The data are presented in Table A-14 and A-15 in App. A. Figures A-39 and A-40 in App. A show the concentration of 2CP at different locations within the column over time.

Based on the release of chloride detected during the batch kinetic experiments, it is assumed that removal of 2CP within the column is the result of microbial degradation. The high background chloride concentration within the soil column prevented the independent determination of the release of chloride in the column.

The first data set indicates that the column was approaching equilibrium after a period of about 300 hours. However, as is shown in Figure A-39 in App. A, the concentrations within the column increased abruptly before equilibrium was reached. The reason for the failure of the column at this point is discussed below. Despite the column failure, steady state concentrations at ports 1, 3, and 5 of the column were estimated by visually extrapolating the data on Figure A-39. Steady state concentrations at port 1, 3, and 5 are estimated as 3.0, 2.0, and 1.35 mg/l, respectively.

The initial failure of the column after 300 hours of good results was suspected to be the result shocking the microorganisms with an ill advised increase in the flow rate from around 4.5 to about 6.5 ml/min. After initial failure, the column was kept running at the higher flow rate to see if it would recover. The only change within the first 5 days appeared to be the build up of microorganisms around the inlet as indicated by decreasing

concentrations at port 1. No significant change was observed at other locations. There appeared to be no biological activity other than at the inlet. In an attempt to remedy this, the flow rate was reduced back to around 4.5 ml/min, and the column was inverted. The theory was that the active microorganisms, which were now at the column exit, would move toward the inlet where the 2CP and oxygen concentrations were higher and redistribute themselves throughout the column. This appeared to work for the first three days as indicated by decreases in 2CP concentrations throughout the length of the column. However, after the fourth day, once again it appeared that the only biological activity was at the inlet. At this point the flow rate was increased in an effort to distribute the microorganisms over a greater length of the column. The column was allowed to run at the higher flow rate for nine days with no apparent improvement.

The column was eventually reseeded with an active culture grown in a batch reactor. After reseeding, the column was subjected to a constant feed concentration of around 6 mg/l of 2CP at a flow rate of about 4.5 mg/l similar to the conditions which were used to obtain the first set of data. As shown in Figure A-40 in App. A, the second trial appeared to reach equilibrium much quicker than the first trial. The equilibrium concentrations of 2CP at ports 1, 3, and 5 from Figure A-40 are 3.29, 1.36, and 0 mg/l respectively. The column appeared to perform at equilibrium for 3 to 4 days. At that point, the concentrations in the column began to increase until it appeared that there was only biological activity at the inlet. After a period of two weeks, the column still had not recovered.

The reason the soil column could not sustain equilibrium in either of the trials is unknown. A possible (?) explanation could be the build up of toxic byproducts which, for some reason, could not be removed from the system.

The degradation of all 6 mg/l of 2CP during the second trial appeared to contradict the aforementioned oxygen limitation. As discussed in chapter 5, section 5.6.3, oxygen saturated medium only contains enough oxygen to degrade 4.76 mg/l of

2CP within the column. The complete degradation of 6 mg/l may indicate that anaerobic degradation may also have been present in the column. Whether the acclimated microorganisms were capable of aerobic and anaerobic degradation of 2CP was not investigated during this study.

Two different steady states were reached in the two continuous flow columns under similar conditions. This may have been the result of the use of a mixed culture. Each culture was grown in a batch reactor prior to seeding. Different conditions during the growing period may have resulted in differences in the composition of the population which was eventually seeded. Different compositions of the mixed culture may have resulted in the different steady states and rates at which they were achieved.

Table 4 Experimental values for model input parameters

Symbol	Parameter	Experimental Value
Y	yield coefficient	0.3 mg biomass/mg 2CP
$\hat{\mu}$	Andrews' parameter	0.26 hr^{-1}
K_s	Andrews' parameter	35 mg/l
K_i	Andrews' parameter	13 mg/l
k_d	adsorption rate constant	0.01227 hr^{-1}
k_p	Freundlich parameter	0.0196 l solvent/g soil
ε_a	void fraction within the aggregate	0.187
ε	void fraction within the mobile phase	0.108
D_{le}	axial diffusion coefficient	4.48 $x10^{-3}$ cm^2/sec

6.6 Predicted Concentrations versus Experimental Data

The values of all experimentally determined parameters for input into the model are presented in Table 4. In addition, the experimental steady state concentrations of 2CP within the soil column are presented in Table 5.

As discussed in chapter 4, the engineering model developed by Lewandowski and Dikshitulu was greatly simplified and solved for steady state biodegradation at low concentrations. The solution is expressed as:

$$\ln\left(\frac{C_b}{C_{bo}}\right) = -\left[\frac{1}{V_z}\left(\frac{\hat{\mu}b}{K_s Y} + k_d\right)\right]z \qquad (6.20)$$

Equation 6.20 can be used to predict the steady state concentration at a given distance, z, in the soil column.

The values of $\hat{\mu}$, K_s, Y, and k_d are presented in Table 4. The flow velocity, V_z, is the length of travel divided by residence time. Using the mean residence time between ports 1 and 5 for the flow rate of 4.45 ml/min which was determined during the tracer studies, V_z is calculated as 0.84 cm/min or 50 cm/hr. The average initial concentration, C_{bo}, for the first and second set of data from the continuous flow column studies are 5.88 and 5.64 mg/l, respectively. These values were determined by averaging the feed tank concentrations at the time the ports were sampled (Table A-14 and A-15 in App. A).

The biomass concentration, b, within the column was not determined. Initially, a constant biomass concentration was assumed by using the experimental steady state concentrations and equation 6.20 to estimate the steady state biomass concentration at each of the measured column ports. The resulting biomass concentrations for the two set of continuous flow column data are presented in Table 5. The calculated biomass concentrations were then averaged. The average biomass concentration was then plugged back into equation 6.20 to predict the steady state concentrations resulting from a constant biomass concentration throughout the column. The results are presented in Table 5. The correlation between the predicted and experimental values is poor.

Without independent measurements of the biomass concentration at different locations within the column, it was not possible to evaluate the accuracy of the model and the assumptions made to obtain a steady state solution. However, assuming that equation 6.20 represents an accurate model of the steady state conditions, the results indicate that the biomass is not evenly distributed over the length of the column. The results from both data sets indicate that more microorganisms are present near the inlet, and they

decrease in concentration over the length of the column. This conclusion seems reasonable since the microorganisms will have a higher growth rate closer to the substrate source, and, furthermore, were seeded via the feed pump.

Using the estimated average biomass concentrations from Table 5, the kinetic term within the parentheses of equation 6.20 is calculated to be 6.5 and 8.2 hr^{-1} for the two data sets. The adsorption term, on the other hand, is 0.01227 hr^{-1}. This shows that the adsorption term is two orders of magnitude less than the kinetic term and plays a minor role in the overall removal process. This seems reasonable based on the hydrophilic nature of 2CP and the lack of humic substances in the synthetic soil.

Table 5 Comparison of experimental values and model-predicted values

Distance in z direction	Experimental steady state concentration (mg/l)	Calculated biomass concentration, b, using equation 6.20 (mg/l)	Predicted steady state concentration using average b and equation 6.20 (mg/l)
		Data Set 1	
2 cm (port 1)	3.00	679	4.23
12 cm (port 3)	2.00	181	0.82
22 cm (port 5)	1.35	135	0.16
		Average b = 332	
		Data Set 2	
2 cm (port 1)	3.29	544	4.34
12 cm (port 3)	1.30	246	1.18
22 cm (port 5)	0	0	0.32
		Average b = 263	

CHAPTER 7

CONCLUSIONS AND RECOMMENDATIONS

It is apparent that more research needs to be done in order to evaluate the proposed in-situ bioremediation engineering model. Many of the model parameters related to the soil characteristics which were determined during this research may be useful in future research. However, it is recommended that a pure culture be used in future kinetic and soil column studies to avoid the problems of working with a mixed culture.

Batch kinetic studies showed that the acclimated mixed culture exhibited substrate inhibited growth as represented by Andrews' model. However, the use of a mixed culture is believed to have been the cause of poor correlation between experimental kinetic data and the Andrews model. In addition, it is believed that the use of a mixed culture was the reason two different steady states were achieved in the soil column experiments despite similar conditions.

Furthermore, in the absence of natural organic matter (humic substances), rates of adsorption to soil, even with 10% clay, were very slow, and negligible compared to the rate of biodegradation. In order to obtain appropriate rates that are more characteristic of field expectations, real soils may have to be used.

In general, experiments with soils and inoculated soil columns are much more difficult to run than suspended growth reactors. The additional complexity increases data scatter, and requires further refinement of experimental techniques.

APPENDIX A

LIST OF SUPPLEMENTARY TABLES AND FIGURES

Table A-1 Results of kinetic run 1

Time (hours)	Optical Density (UOD)	Biomass Concentration (ppm)	2-Chlorophenol Concentration (ppm)
0.000	0. 034	9.30	17.92
0.500	0. 035	9.57	13.66
1.000	0. 034	9.30	13.75
1.416	0. 037	10.12	14.05
1.916	0. 038	10.39	11.94
2.416	0. 039	10.66	10.99
2.916	0. 038	10.39	9.79
3.416	0. 041	11.21	8.28
3.916	0. 042	11.48	6.82
4.416	0. 042	11.48	4.19
4.916	0. 045	12.30	2.95

Table A-2 Results of kinetic run 2

Time (hours)	Optical Density (UOD)	Biomass Concentration (ppm)	2-Chlorophenol Concentration (ppm)
0.00	0. 076	20.78	29.50
0.50	0. 079	21.60	25.68
1.25	0. 089	24.33	19.97
1.75	0. 086	23.51	15.73
2.25	0. 088	24.06	12.23
2.75	0. 097	26.52	8.59
3.25	0. 104	28.43	4.68
3.75	0. 105	28.71	1.04
4.25	0. 107	29.25	0.00

Table A-3 Results of kinetic run 3

Time (hours)	Optical Density (UOD)	Biomass Concentration (ppm)	2-Chlorophenol Concentration (ppm)
0.00	0. 130	35.54	42.95
0.50	0. 131	35.81	44.84
1.00	0. 132	36.09	36.16
1.50	0. 140	38.27	35.66
2.00	0. 139	38.00	31.97
2.50	0. 143	39.09	30.52
3.00	0. 163	44.56	27.06
3.50	0. 163	44.56	22.02
4.00	0. 173	47.30	17.35
4.50	0. 180	49.21	11.75
5.00	0. 188	51.40	4.61
5.50	0. 205	56.04	0.00

Table A-4 Results of kinetic run 4

Time (hours)	Optical Density (UOD)	Biomass Concentration (ppm)	2-Chlorophenol Concentration (ppm)
0.00	0. 097	26.52	13.05
0.50	0. 100	27.34	12.29
1.00	0. 104	28.43	11.38
1.50	0. 106	28.98	11.44
2.00	0. 108	29.53	10.14
2.50	0. 110	30.07	8.23
3.00	0. 115	31.44	7.82
4.00	0. 118	32.26	3.60
4.50	0. 122	33.35	3.26
5.00	0. 126	34.45	1.82
5.50	0. 126	34.45	0.82

Table A-5 Results of kinetic run 5

Time (hours)	Optical Density (UOD)	Biomass Concentration (ppm)	2-Chlorophenol Concentration (ppm)
0.00	0. 168	45.93	45.67
0.50	0. 175	47.84	39.63
1.00	0. 180	49.21	36.04
1.50	0. 189	51.67	27.62
2.00	0. 210	57.41	15.20
2.50	0. 226	61.78	8.37
3.00	0. 243	66.43	0.00

Table A-6 Results of kinetic run 6

Time (hours)	Optical Density (UOD)	Biomass Concentration (ppm)	2-Chlorophenol Concentration (ppm)
0.00	0. 049	13.40	57.01
1.00	0. 052	14.22	51.91
2.00	0. 053	14.49	48.33
3.00	0. 058	15.86	46.72
4.00	0. 060	16.40	38.69
5.00	0. 063	17.22	31.18
6.00	0. 068	18.59	29.44
7.00	0. 070	19.14	21.22

Table A-7 Results of kinetic run 7

Time (hours)	Optical Density (UOD)	Biomass Concentration (ppm)	2-Chlorophenol Concentration (ppm)
0.00	0. 115	31.44	100.60
1.00	0. 115	31.44	90.92
2.00	0. 115	31.44	84.79
3.00	0. 115	31.44	84.57
4.00	0. 118	32.26	77.34
5.00	0. 124	33.90	71.53
6.00	0. 121	33.08	56.02
7.00	0. 126	34.45	56.86
8.00	0. 128	34.99	44.33
8.33	0. 135	36.91	43.27
9.00	0. 136	37.18	38.81

Table A-8 Results of kinetic run 8

Time (hours)	Optical Density (UOD)	Biomass Concentration (ppm)	2-Chlorophenol Concentration (ppm)
0.00	0. 082	22.42	56.88
0.50	0. 083	22.69	53.36
1.00	0. 084	22.96	52.60
1.50	0. 085	23.24	51.12
2.00	0. 086	23.51	49.08
2.50	0. 088	24.06	47.00
3.00	0. 090	24.60	45.82
3.50	0. 092	25.15	43.12

Table A-9 Results of kinetic run 9

Time (hours)	Optical Density (UOD)	Biomass Concentration (ppm)	2-Chlorophenol Concentration (ppm)
0.00	0. 116	31.71	70.08
1.00	0. 118	32.26	66.24
1.50	0. 122	33.35	67.62
2.00	0. 127	34.72	66.93
2.50	0. 130	35.54	64.33
3.50	0. 136	37.18	57.84
4.00	0. 139	38.00	52.16
4.50	0. 141	38.55	50.33
5.00	0. 143	39.09	44.82
5.50	0. 151	41.28	42.77
6.00	0. 157	42.92	42.60

Table A-10 Results of kinetic run 10

Time (hours)	Optical Density (UOD)	Biomass Concentration (ppm)	2-Chlorophenol Concentration (ppm)
0.00	0. 097	26.52	52.22
1.00	0. 091	24.88	48.31
2.00	0. 098	26.79	45.11
2.50	0. 101	27.61	44.53
3.50	0. 108	29.53	34.11
4.50	0. 116	31.71	29.38
6.00	0. 129	35.27	18.39
6.25	0. 143	39.09	15.74
7.00	0. 162	44.29	12.21

Table A-11 Results of kinetic run 11

Time (hours)	Optical Density (UOD)	Biomass Concentration (ppm)	2-Chlorophenol Concentration (ppm)
0.00	0. 050	13.67	70.08
1.00	0. 053	14.49	67.29
2.00	0. 053	14.49	65.16
3.00	0. 054	14.76	60.32
4.00	0. 056	15.31	57.49
5.00	0. 058	15.86	51.41
6.00	0. 060	16.40	45.59
7.00	0. 060	16.40	39.70
7.50	0. 061	16.68	38.78

Table A-12 Results of batch adsorption experiments

Initial experiment		Confirmatory Experiments						
Sample size	15 g soil		15 g soil		22.5 g soil		30 g soil	
Time (hours)	Conc. of 2CP in solution(mg/l) Experimental	Time (hours)	Concentration of 2CP in solution (mg/l) Experimental	Predicted	Concentration of 2CP in solution (mg/l) Experimental	Predicted	Concentration of 2CP in solution (mg/l) Experimental	Predicted
0	7.16	0	6.2	7.59	6.2	7.16	6.2	6.91
19	6.72	6	6.18	7.16	6.22	6.74	6.29	6.49
21.66	6.63	22	6.11	6.17	6.15	5.74	6.03	5.49
25	5.99	29	5.94	5.79	5.87	5.36	5.88	5.11
44	5.84	46	5.08	4.99	4.91	4.57	4.59	4.32
67.5	4.45	52	4.97	4.75	4.71	4.33	4.51	4.08
164	2.63	70	4.65	4.12	4.52	3.70	4.04	3.45
187.5	2.4	77	4.43	3.91	4.31	3.49	3.83	3.24
211.5	2.18	94	4.42	3.47	3.61	3.05	2.53	2.80
235	1.97	99.5	4.41	3.35	3.14	2.92	1.74	2.67
331.5	1.82	115	4.3	3.04	0	2.62	0	2.37
379	1.82							

Notes: $C = 6.012 \exp(-0.01227t) + C^*$

$C^* = q/k_p$

$k_p = 19.6$ l solvent/kg soil

Table A-13 Results of chloride tracer experiments

Flow = 0.085 ml/min		Flow = 1.05 ml/min		Flow = 4.45 ml/min				
Time (min)	Chloride Concentration[1] (mg/l)	Time (min)	Chloride Concentration[1] (mg/l)	Time (min)	Trial 1 Chloride Concentration[1] (mg/l)	Trial 2 Chloride Concentration[1] (mg/l)	Trial 3 Chloride Concentration[1] (mg/l)	Average Chloride Concentration[1] (mg/l)
0	0	0	0	0	0	0	0	0
45	0.01	70	0.01	5	0	0	0	0
50	0.05	80	0.28	10	0	0	0	0
60	0.03	85	0.52	15	0.29	0.61	0.66	0.52
66	0.12	90	0.66	17.5	-	-	2.16	2.16
70	0.18	95	0.92	20	2.57	3.62	3.25	3.15
75	0.66	100	1.02	22.5	-	2.99	3.13	3.06
80	0.74	105	1.26	25	2.10	2.49	2.75	2.45
85	1.03	110	1.18	30	0.95	1.45	1.81	1.40
90	1.26	120	0.91	35	0.32	0.56	0.76	0.54
95	1.97	125	0.82	40	0	0.22	0.33	0.18
100	1.97	130	0.81	45	0	0	0.03	0.01
105	2.21	145	0.61	50	0	0	0	0
110	2.20	155	0.31	55	0	0	0	0
115	2.05	180	0.26					
120	1.90	205	0.15					
125	2.03	235	0.07[2]					
130	1.80	265	0.04[2]					
135	1.54	295	0.02[2]					
145	1.40							
155	1.11							
170	0.70							
195	0.33							
220	0.16[2]							
245	0.08[2]							
270	0.04[2]							
295	0.02[2]							

Notes: 1 Chloride concentrations have been corrected to remove background chloride levels.
2 Data obtained from extrapolation of data.

Table A-14 - Results of continuous flow column studies - Data set 1

Time	2-Chlorophenol Concentratin (mg/l)				Flow Rate
(hours)	Feed Tank	Port 1	Port 3	Port 5	(ml/min)
0.00					
6.00	5.92	5.50	5.39	5.62	2.20
24.00	5.90	5.44	5.55	5.46	3.50
30.25	5.88	5.19	5.21	5.42	3.00
47.75	5.59	5.22	5.20	5.06	4.20
53.25	5.46	5.00	4.84	4.93	3.20
73.75	5.74	5.03	4.67	4.72	4.90
118.00	5.94	3.87	3.29	3.74	3.30
125.75	5.63	4.22	4.01	3.96	3.10
144.25	5.91	4.04	3.80	3.83	3.00
149.75	5.60	3.14	3.41	3.39	4.20
168.25	6.26	3.84	3.31	3.22	4.60
173.50	5.90	3.93	3.27	3.22	3.90
192.75	6.16	3.44	2.97	2.92	3.84
197.75	5.97	3.67	3.09	2.97	4.40
215.50	6.21	3.71	3.20	2.88	4.55
221.25	5.90	3.43	3.10	2.48	4.33
241.25	5.92	3.66	2.69	1.76	4.65
288.25	5.97	2.91	1.85	1.44	3.70
295.25	5.94	3.04	2.03	1.85	4.65
312.00	6.31	3.76	3.00	2.88	6.75
318.25	5.14	3.38	2.84	2.81	5.15
336.00	5.90	4.06	3.58	3.56	6.17
341.25	5.56	3.90	3.78	3.61	4.93
360.25	5.36	3.70	3.47	3.45	4.93
366.75	4.86	2.98	2.93	3.11	4.75
385.25	5.95	5.66	5.19	4.22	4.28
387.25	5.89	5.74	5.63	4.70	5.15
389.50	5.76	5.58	5.44	4.45	5.00
409.00	5.71	5.38	5.09	2.86	5.05
430.25	5.66	5.39	4.03	0.76	4.80
457.25	5.78	5.46	1.96	1.41	4.25
480.25	4.53	4.08	3.02	3.08	4.43
485.75	5.12	4.57	2.99	3.03	4.40
503.75	5.09	4.87	4.06	4.40	5.70
509.75	5.51	4.78	4.30	4.34	5.25
528.25	5.72	4.71	4.35	4.36	5.18
534.00	5.60	4.43	4.33	4.41	4.40
551.50	6.28	4.65	4.84	4.85	4.60

Note: Column was inverted at 367 hours.

Table A-15 - Results of continuous flow column studies - Data set 2

Time	2-Chlorophenol Concentratin (mg/l)				Flow Rate
(hour)	Feed Tank	Port 1	Port 3	Port 5	(ml/min)
0.00					
4.00	6.07	5.71	5.46	5.55	4.50
25.75	6.00	5.32	5.18	5.05	4.70
71.25	5.68	3.82	1.52	0	4.50
95.00	5.60	3.26	0.95	0	4.53
102.50	5.47	3.24	1.60	0	4.87
119.00	5.84	3.35	1.36	0	4.80
144.00	5.33	2.80	1.29	0.46	4.90
167.50	5.61	3.89	1.66	1.23	4.77
193.50	5.84	4.23	3.78	4.25	4.80
239.00	5.32	4.00	3.68	3.59	4.58
267.50	5.85	4.84	3.45	3.84	4.45
308.00	5.70	3.74	3.62	3.64	4.27
356.75	6.73	6.63	6.68	4.76	3.93
380.75	5.78	4.40	3.74	3.89	3.50
410.00	5.49	3.93	3.33	3.56	4.25

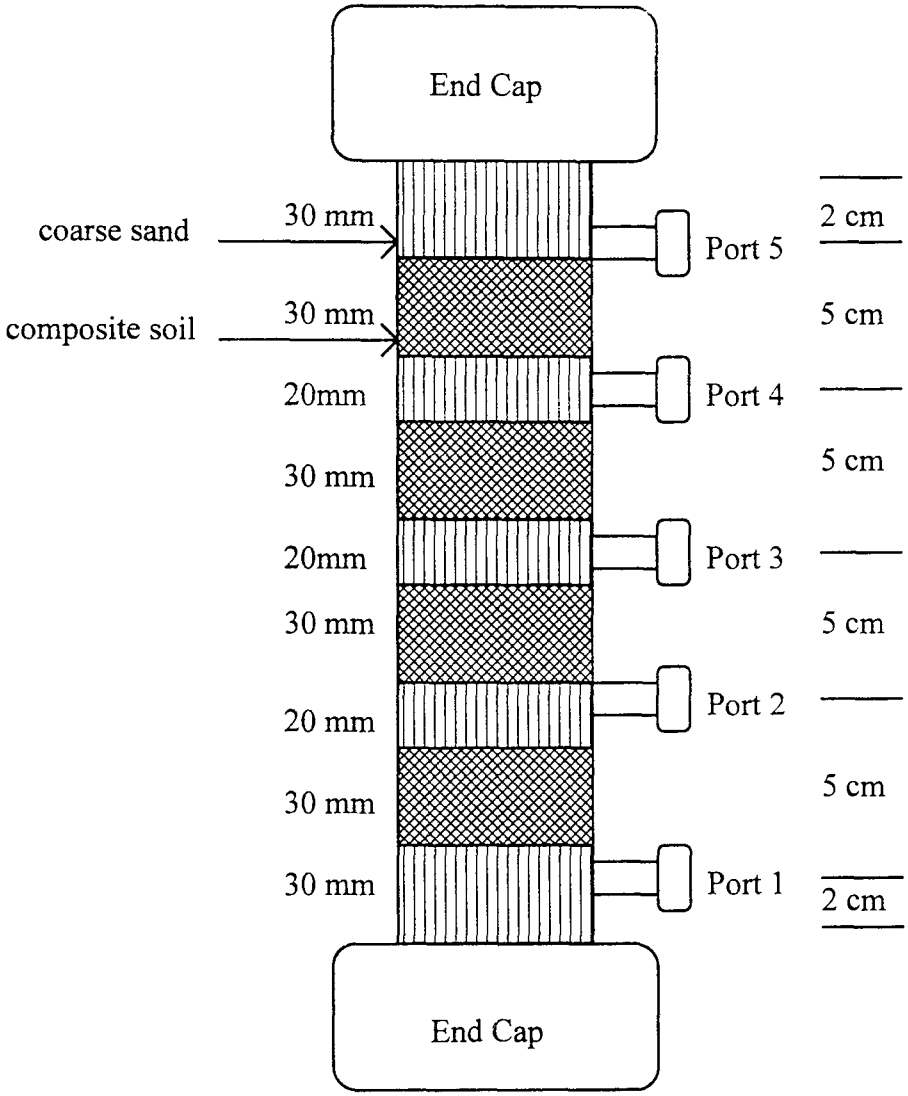

Figure A-1 Details of Column Packing.

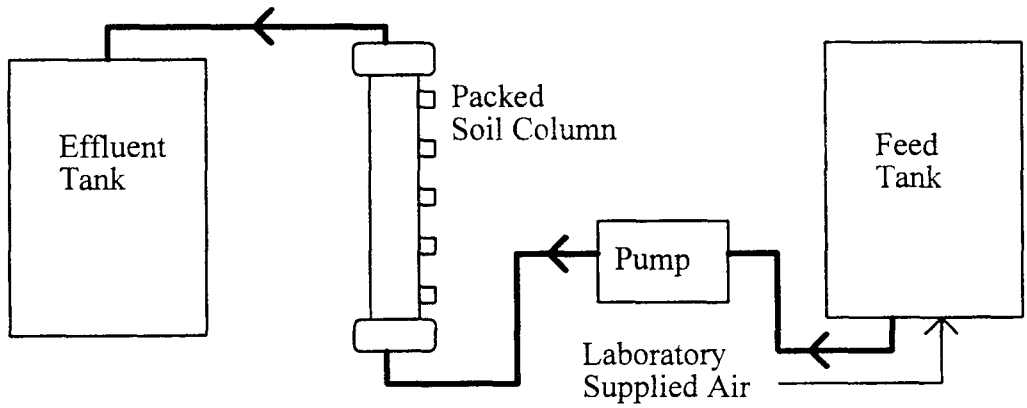

Figure A-2 Schematic diagram of continuous flow column set up.

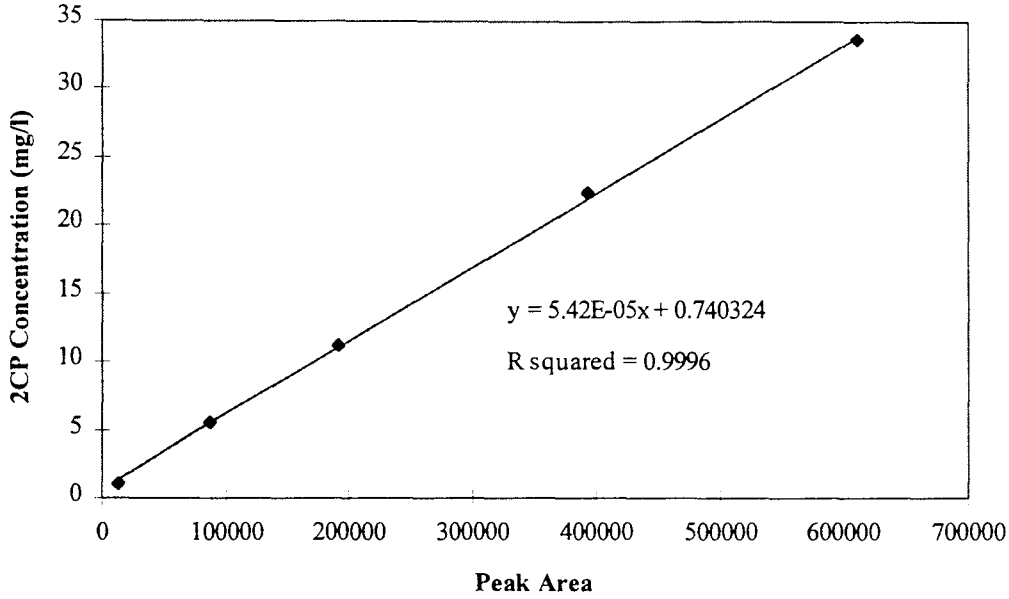

Figure A-3 Typical calibration curve for the determination of the 2-chlorophenol concentration from the areae detected by the HPLC.

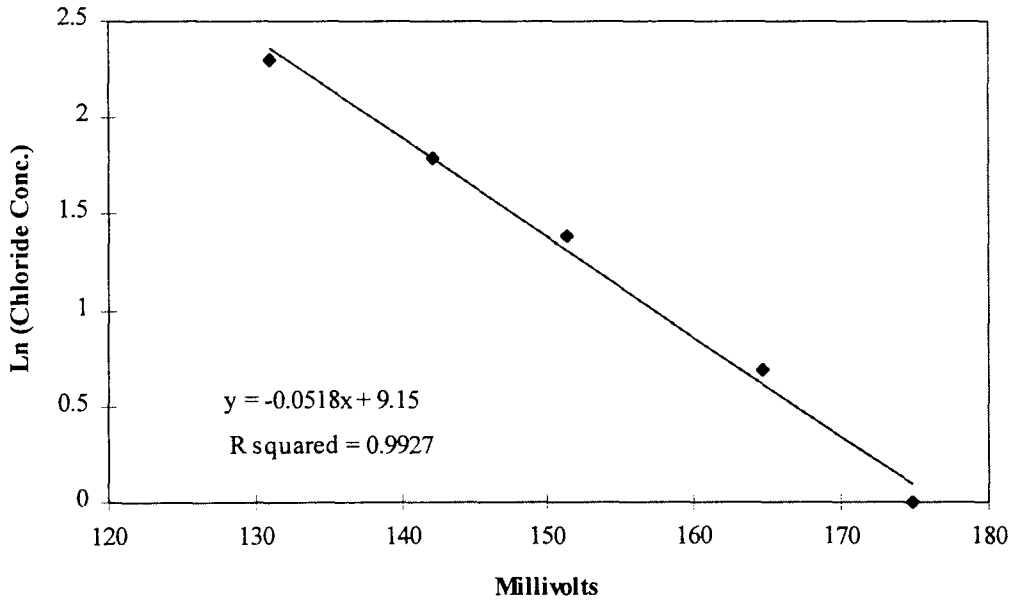

Figure A-4 Typical calibration curve for the determination of the chloride concentration from the millivolt reading.

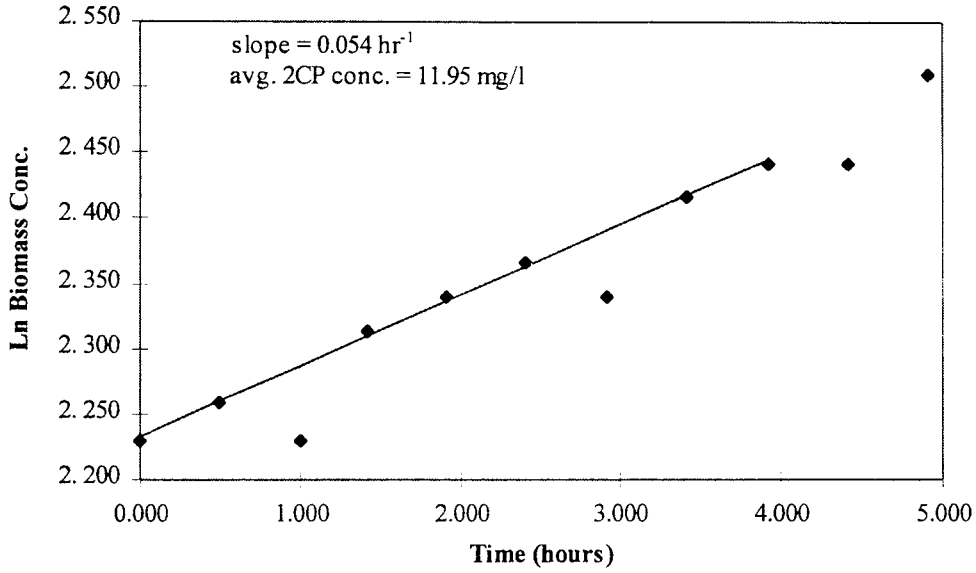

Figure A-5 Run 1: Plot of exponential growth phase to determine specific growth rate.

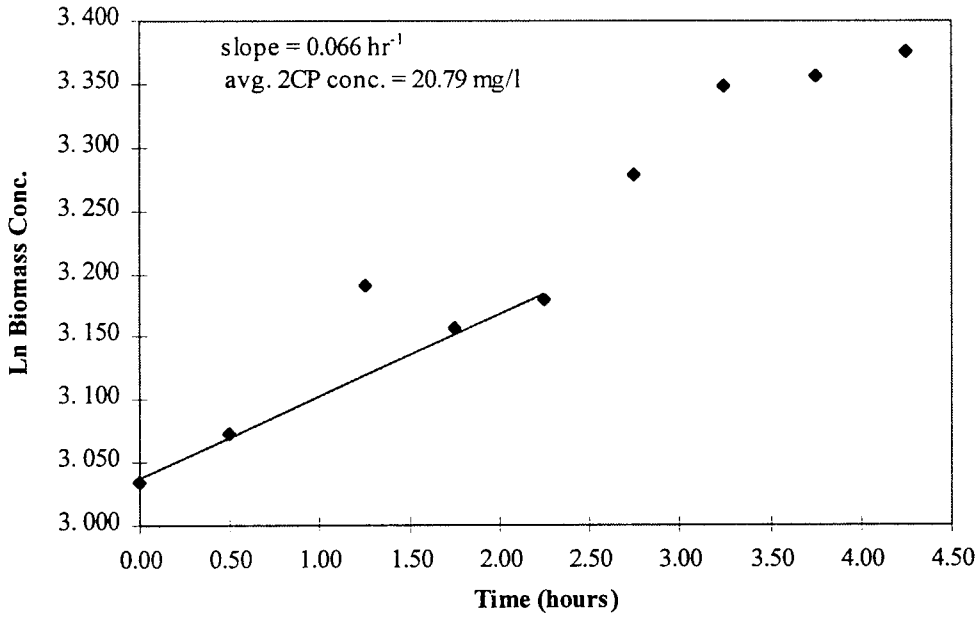

Figure A-6 Run 2: Plot of exponential growth phase to determine specific growth rate.

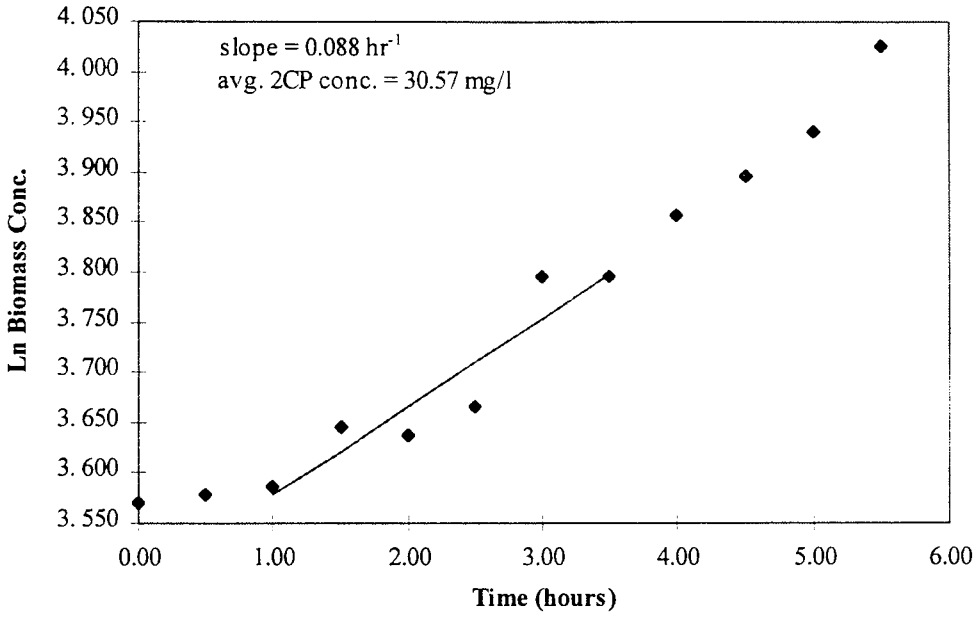

Figure A-7 Run 3: Plot of exponential growth phase to determine specific growth rate.

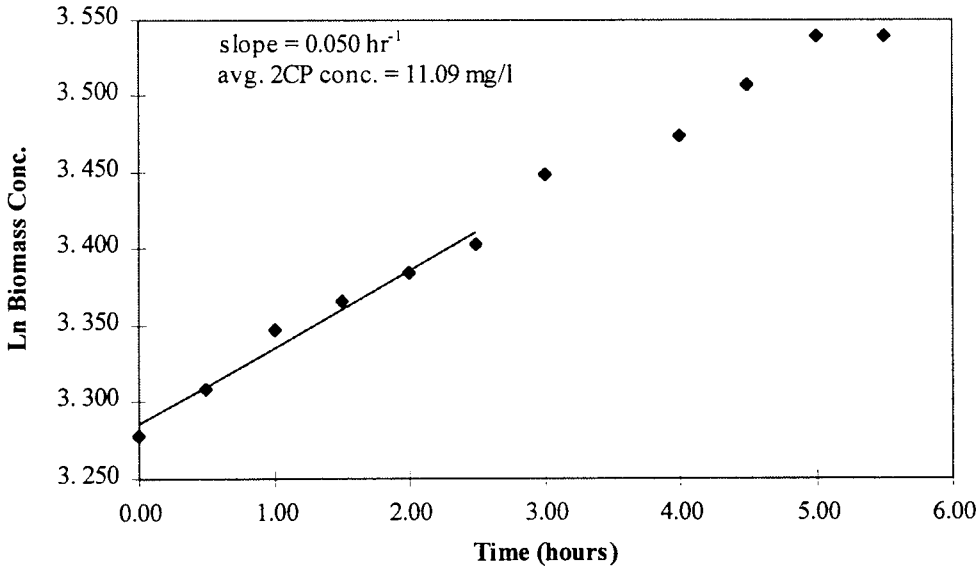

Figure A-8 Run 4: Plot of exponential growth phase to determine specific growth rate.

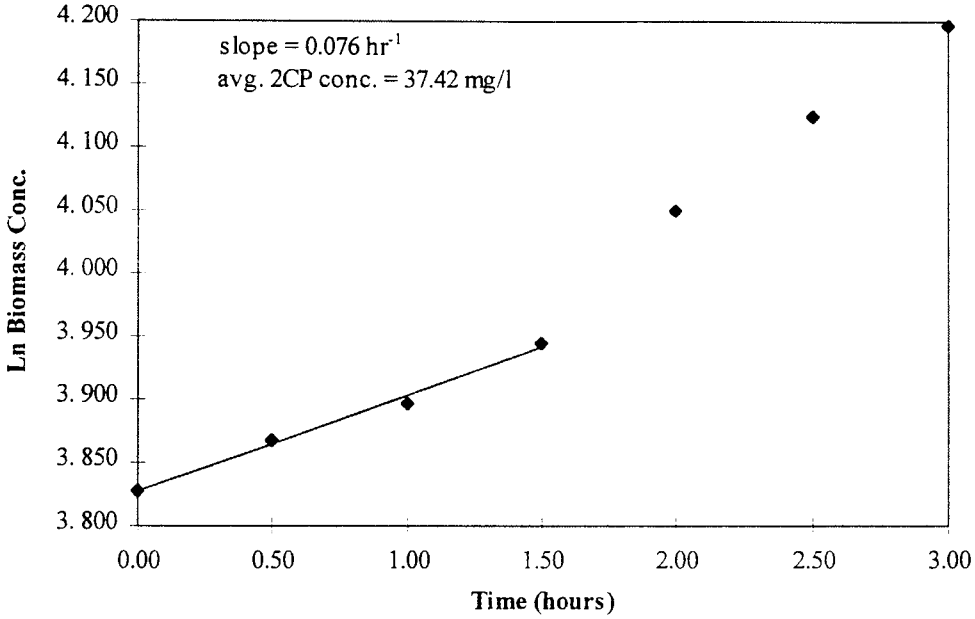

Figure A-9 Run 5: Plot of exponential growth phase to determine specific growth rate.

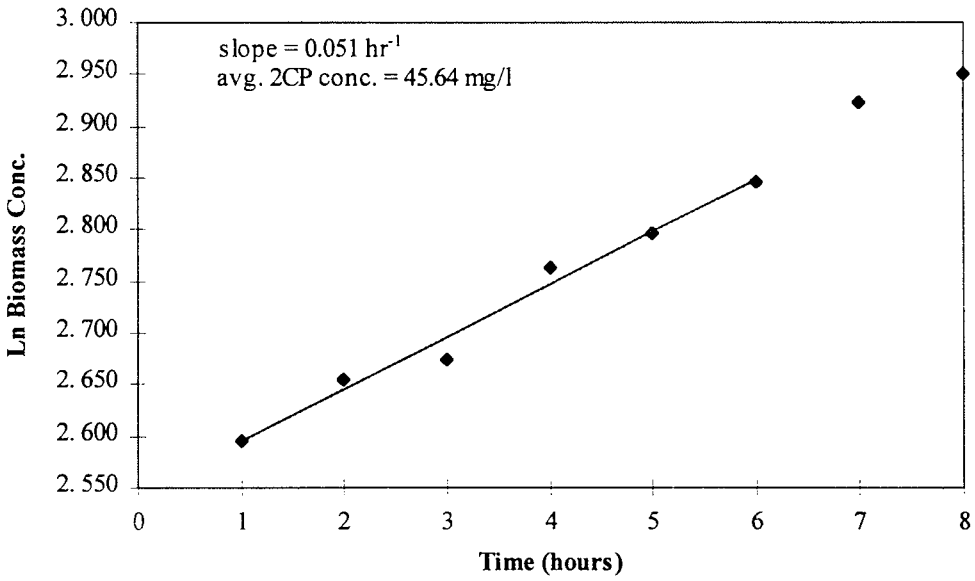

Figure A-10 Run 6: Plot of exponential growth phase to determine specific growth rate.

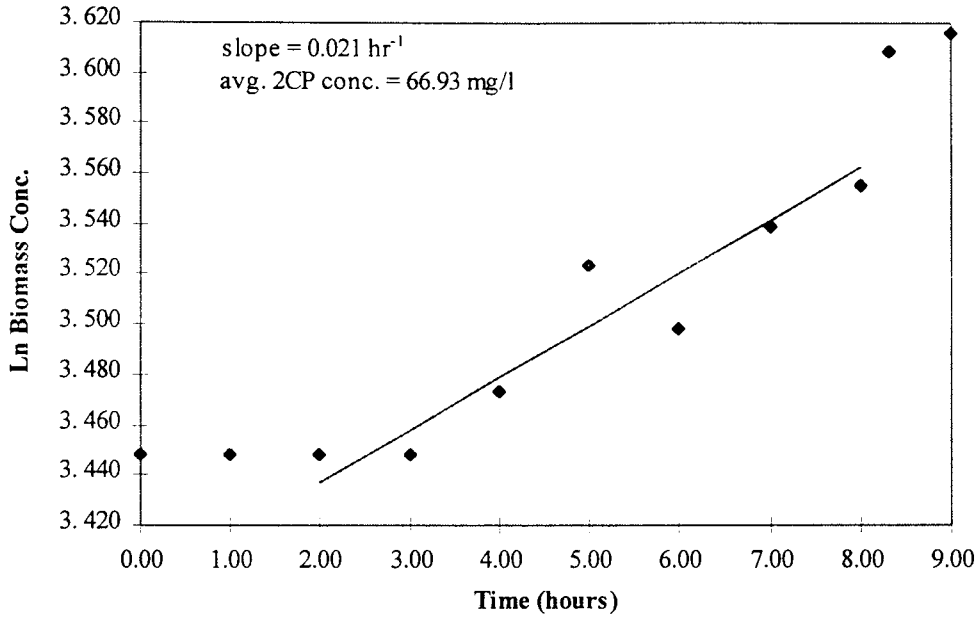

Figure A-11 Run 7: Plot of exponential growth phase to determine specific growth rate.

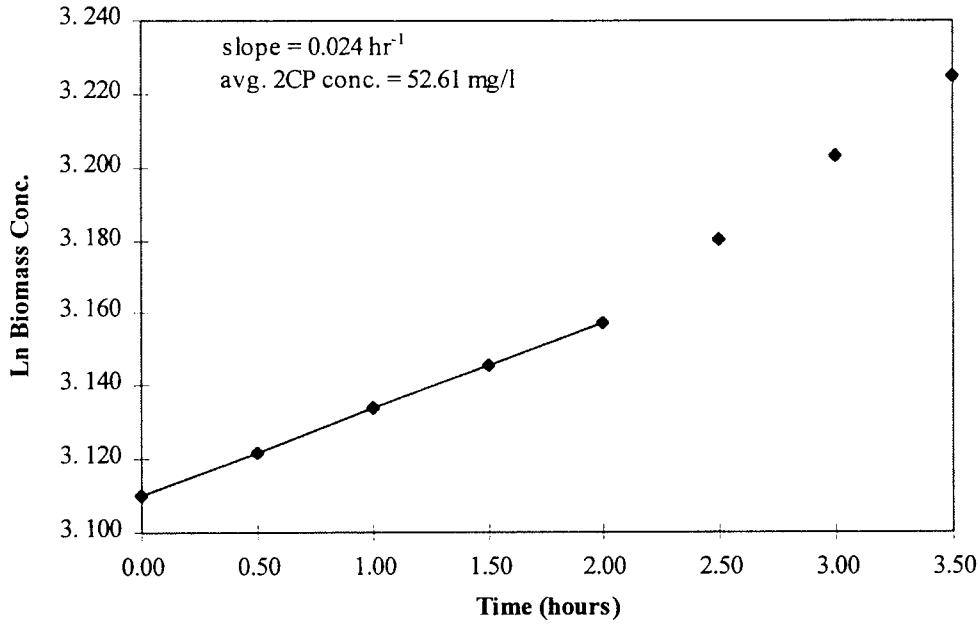

Figure A-12 Run 8: Plot of exponential growth phase to determine specific growth rate.

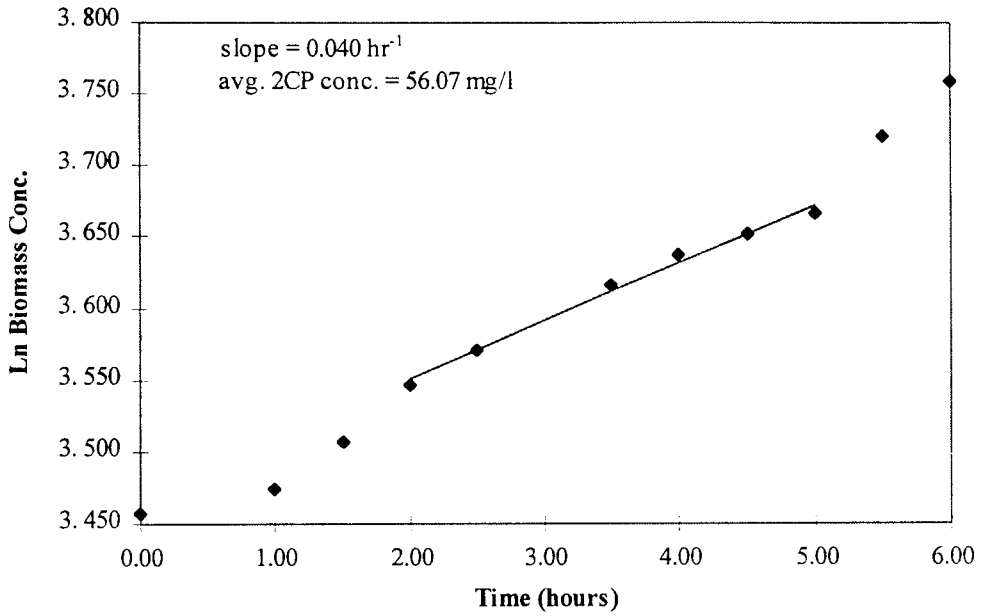

Figure A-13 Run 9: Plot of exponential growth phase to determine specific growth rate.

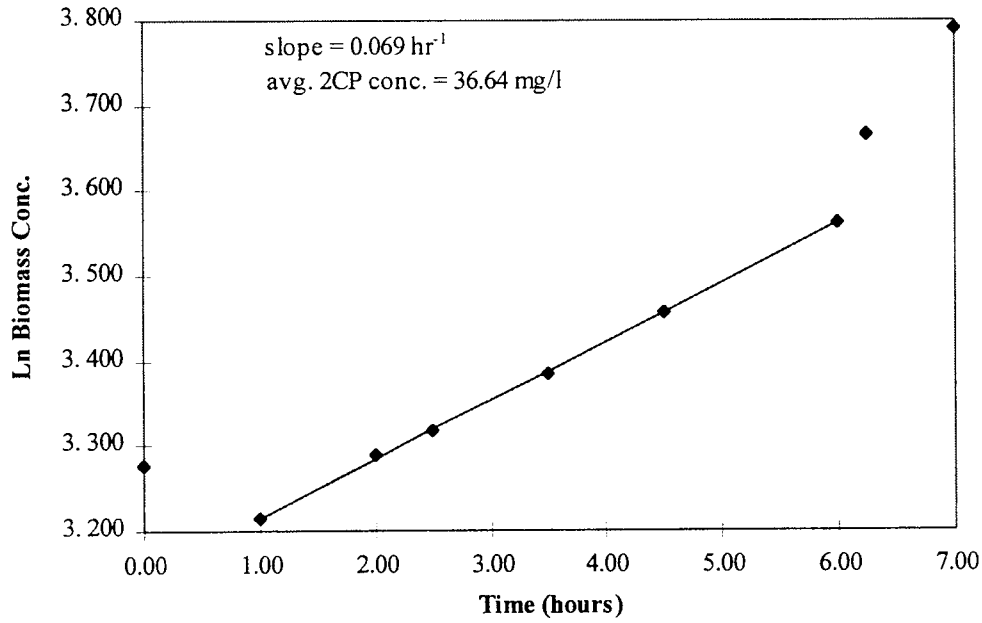

Figure A-14 Run 10: Plot of exponential growth phase to determine specific growth rate.

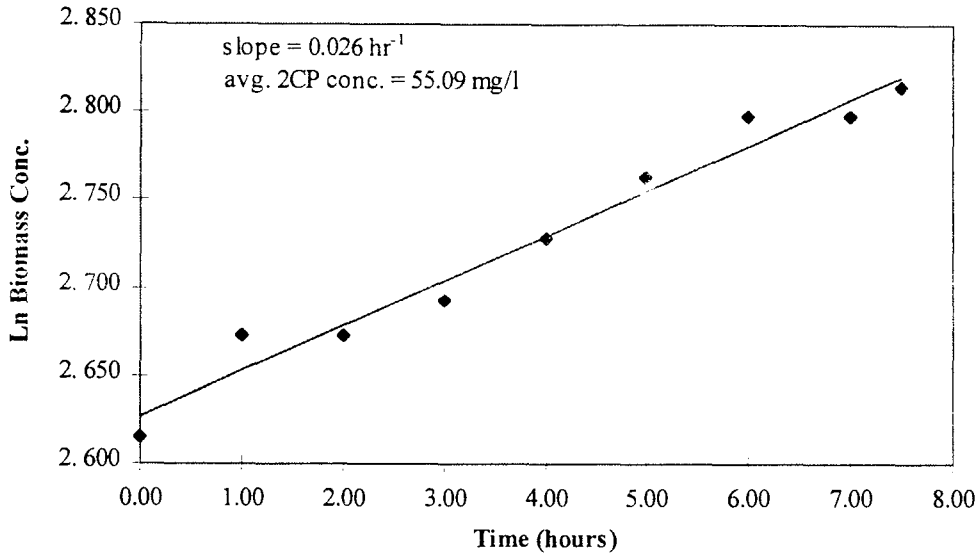

Figure A-15 Run 11: Plot of exponential growth phase to determine specific growth rate.

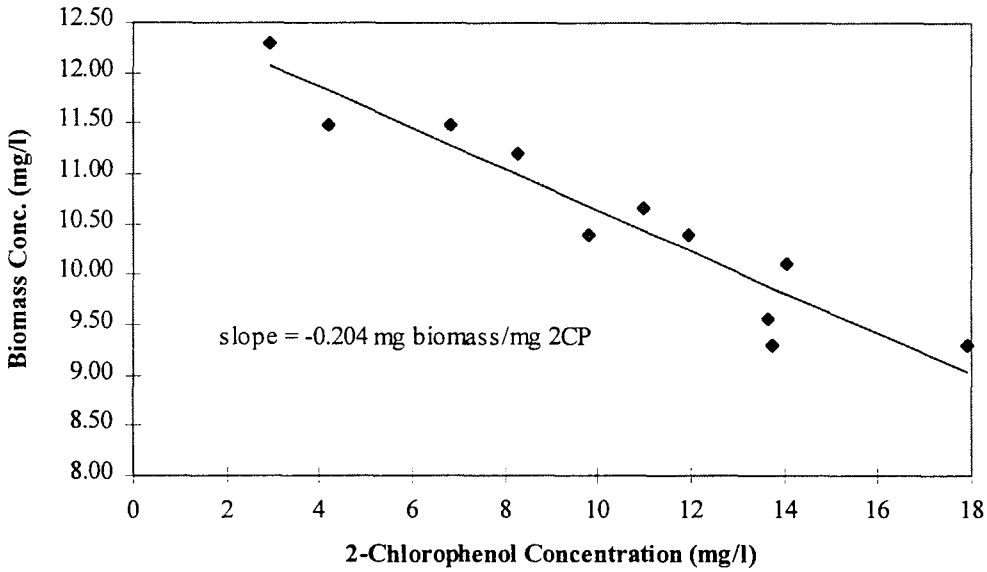

Figure A-16 Run 1: Plot of exponential growth phase to determine yield coefficient.

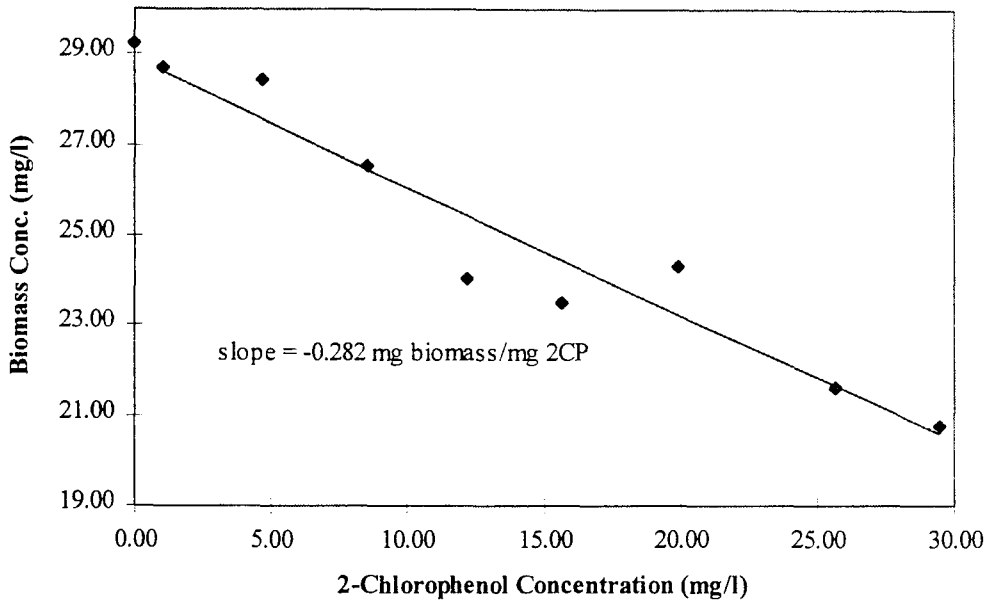

Figure A-17 Run 2: Plot of exponential growth phase to determine yield coefficient.

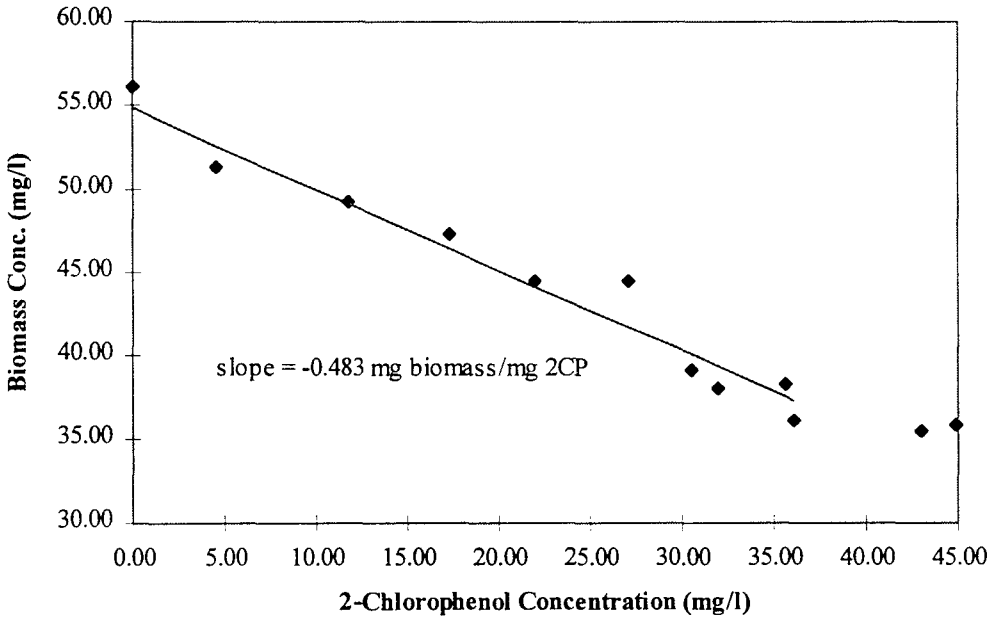

Figure A-18 Run 3: Plot of exponential growth phase to determine yield coefficient.

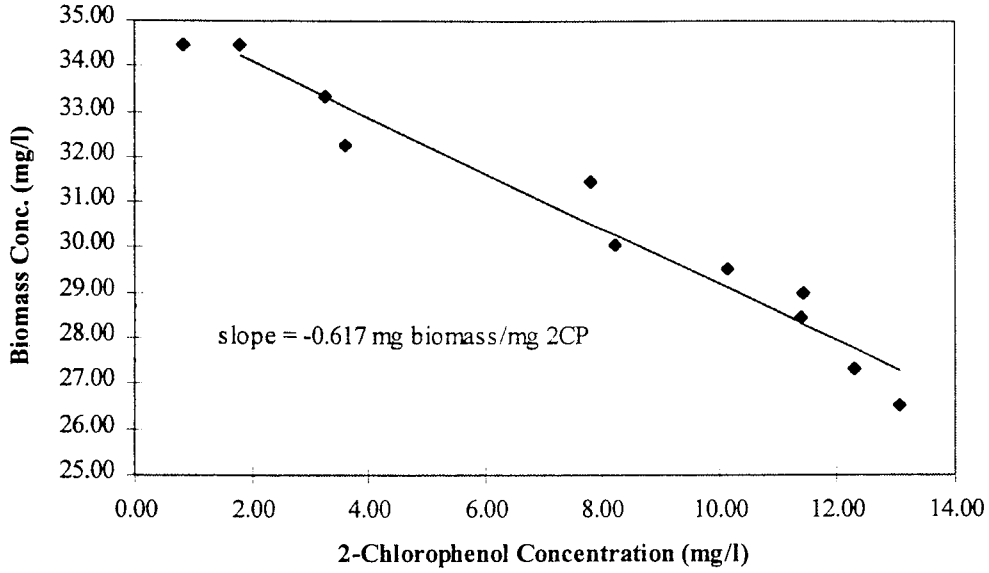

Figure A-19 Run 4: Plot of exponential growth phase to determine yield coefficient.

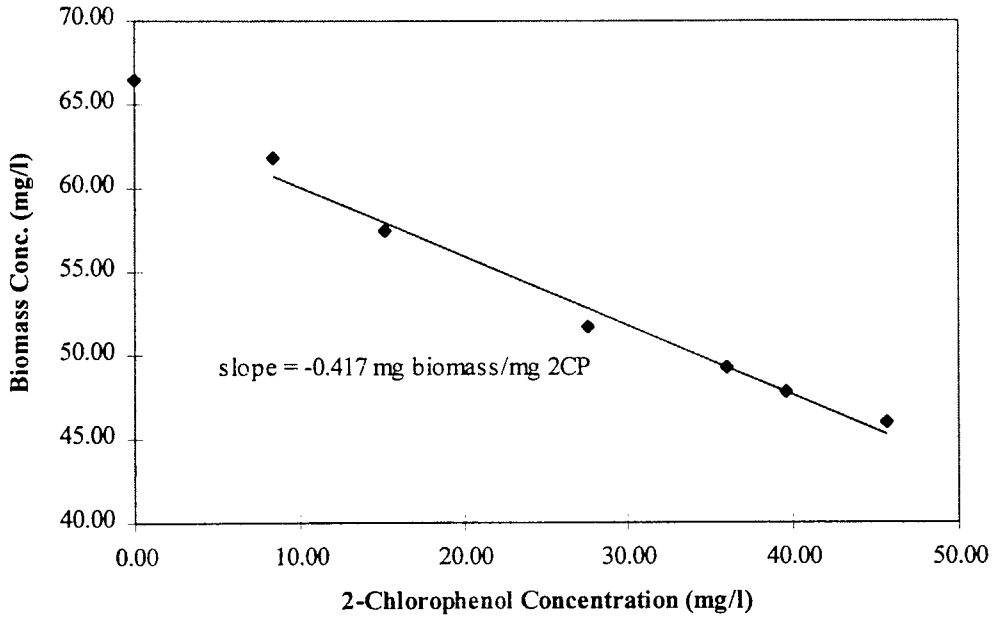

Figure A-20 Run 5: Plot of exponential growth phase to determine yield coefficient.

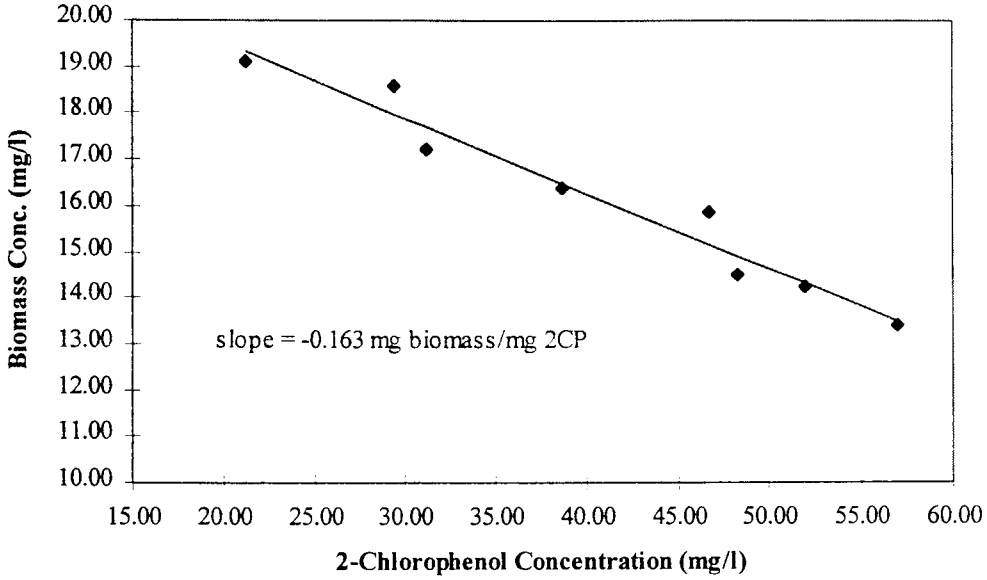

Figure A-21 Run 6: Plot of exponential growth phase to determine yield coefficient.

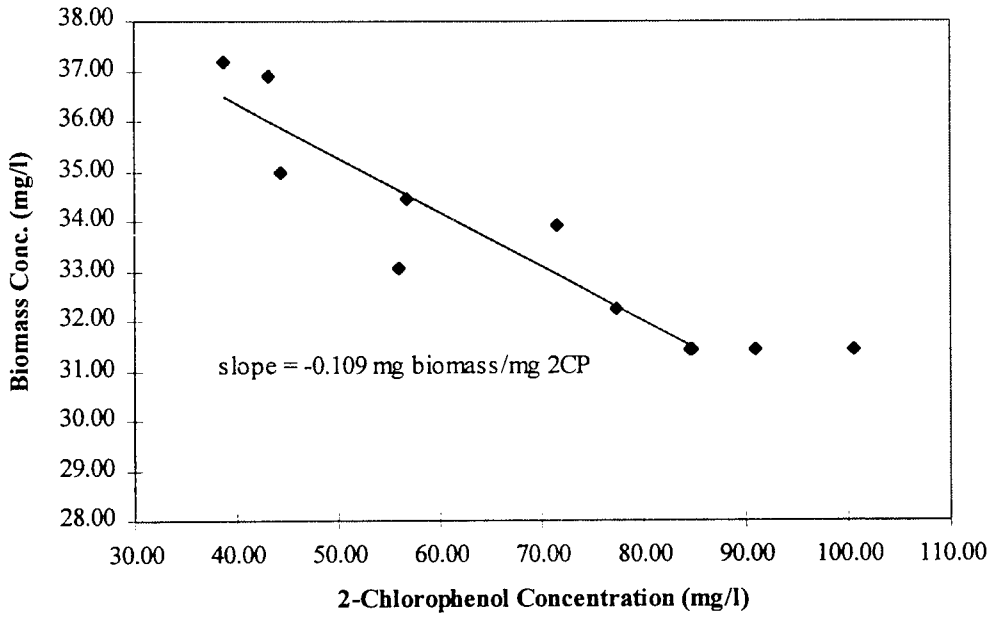

Figure A-22 Run 7: Plot of exponential growth phase to determine yield coefficient.

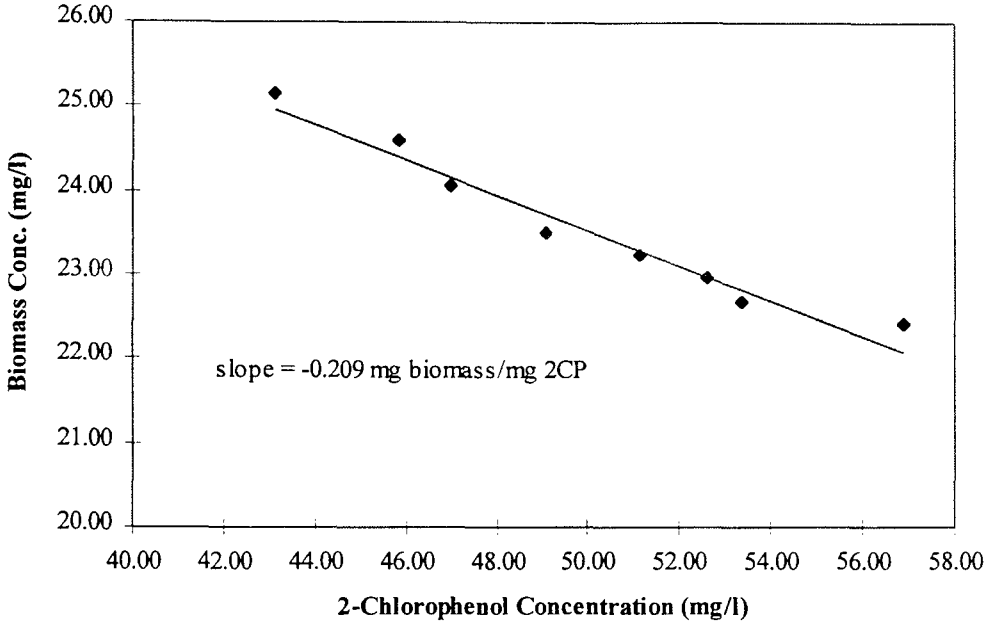

Figure A-23 Run 8: Plot of exponential growth phase to determine yield coefficient.

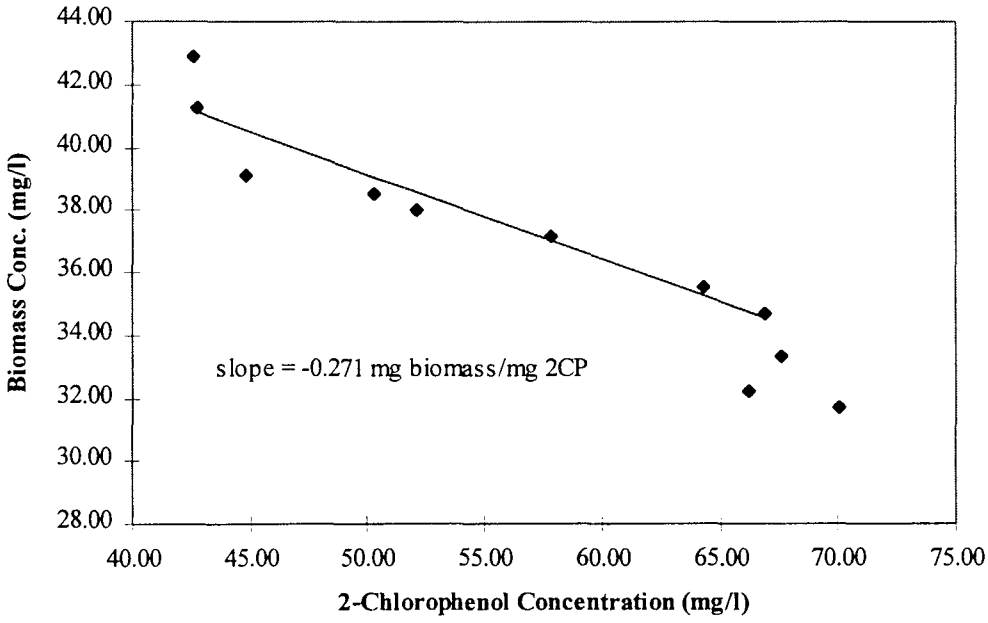

Figure A-24 Run 9: Plot of exponential growth phase to determine yield coefficient.

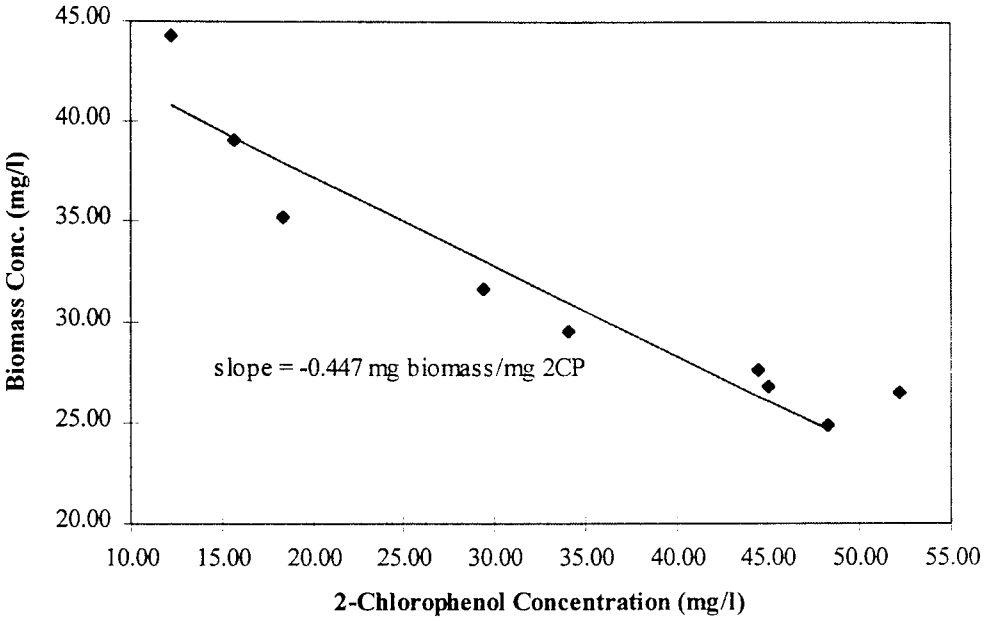

Figure A-25 Run 10: Plot of exponential growth phase to determine yield coefficient.

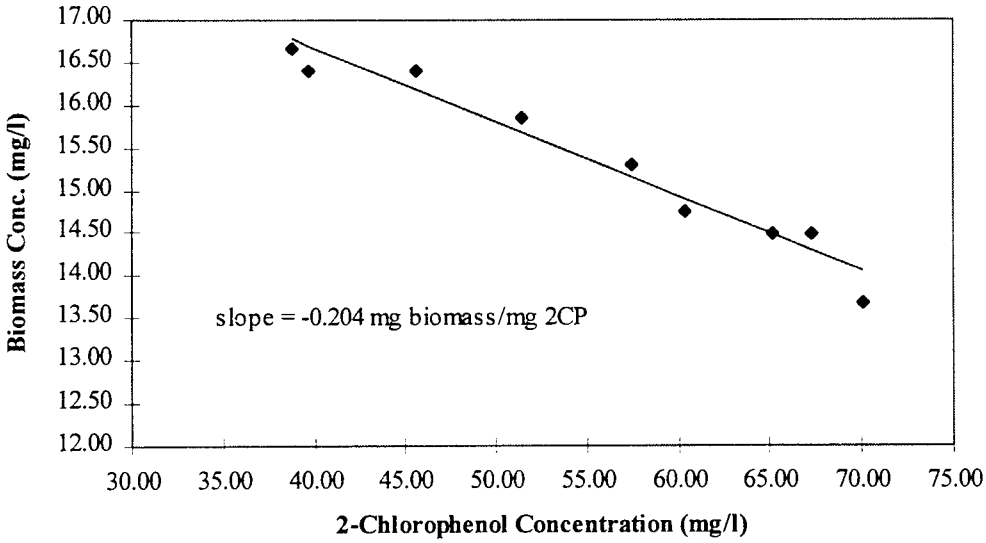

Figure A-26 Run 11: Plot of exponential growth phase to determine yield coefficient.

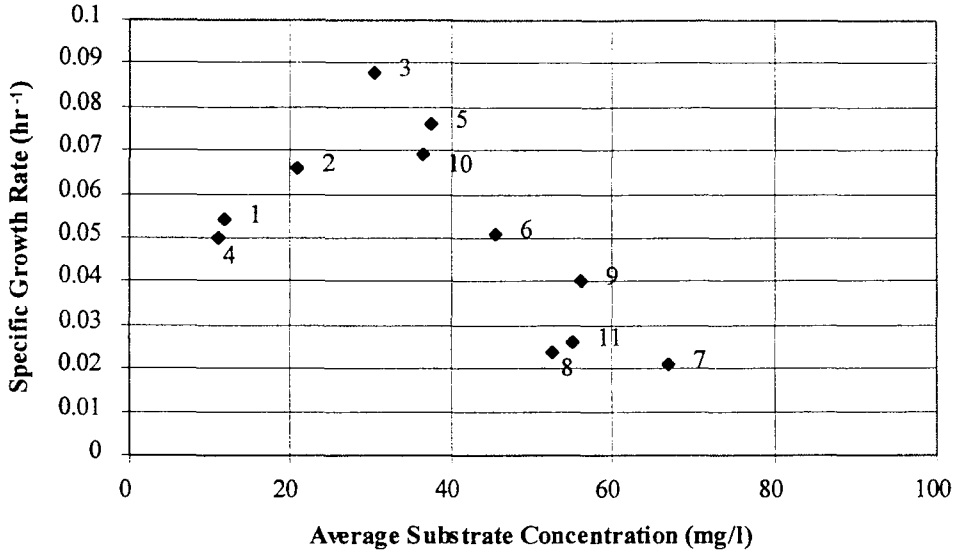

Figure A-27 Specific growth rate versus average 2-chlorophenol concentration for the determination of Andrews Model parameters.

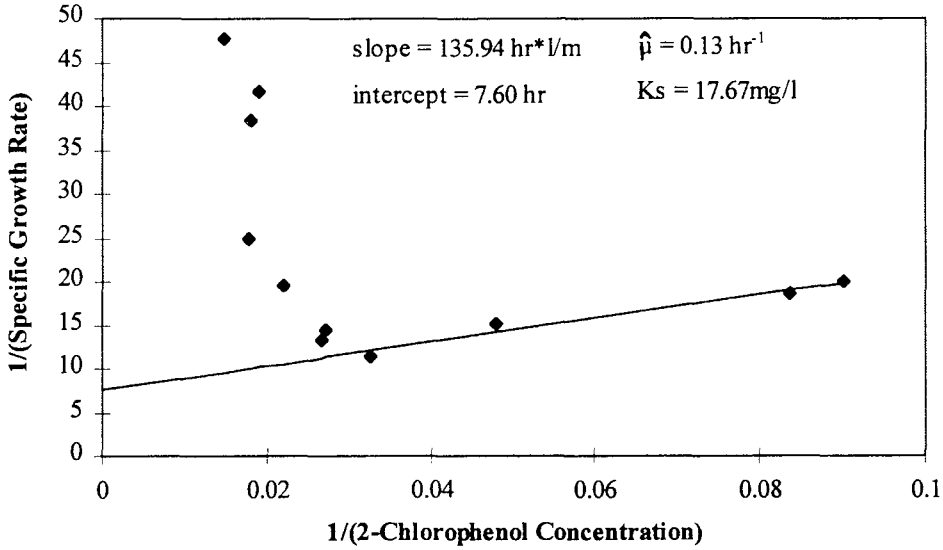

Figure A-28 Plot of $1/\mu$ versus $1/C_a$. Estimation of Andrews Model parameters at low concentrations.

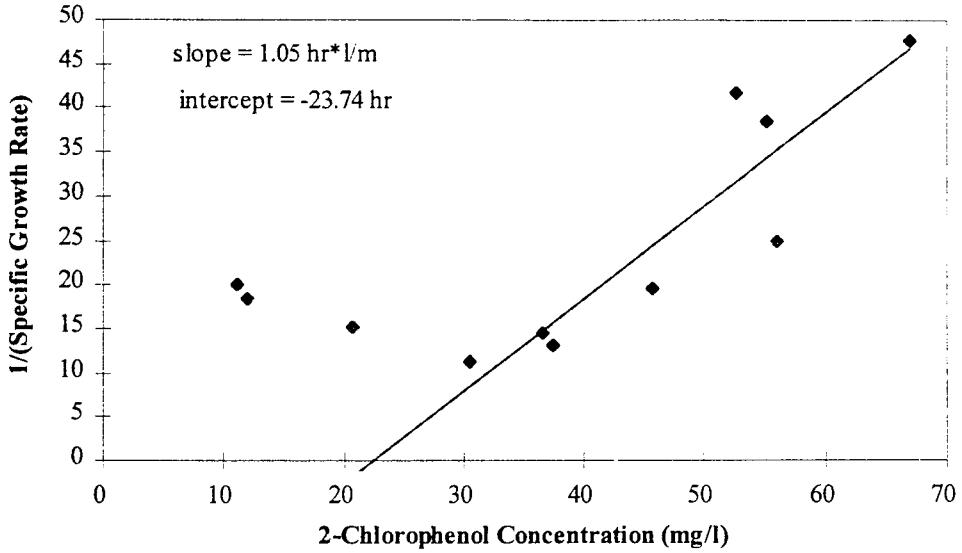

Figure A-29 Plot of $1/\mu$ versus C_a. Estimation of Andrews Model parameters at high concentrations.

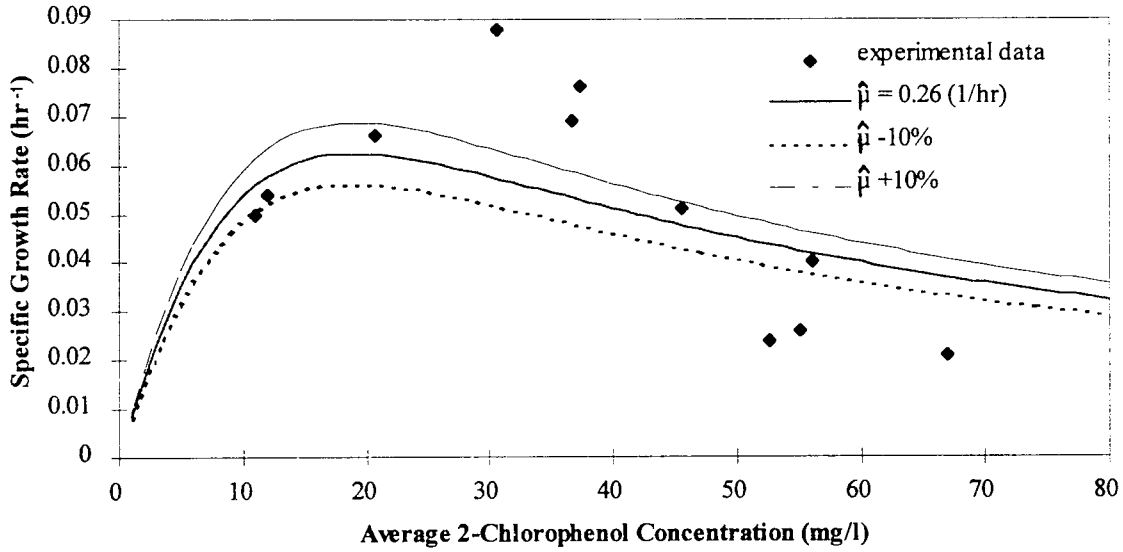

Figure A-30 Growth curve fit using estimated Andrews Model parameters showing results of perturbations of $\hat{\mu}$.

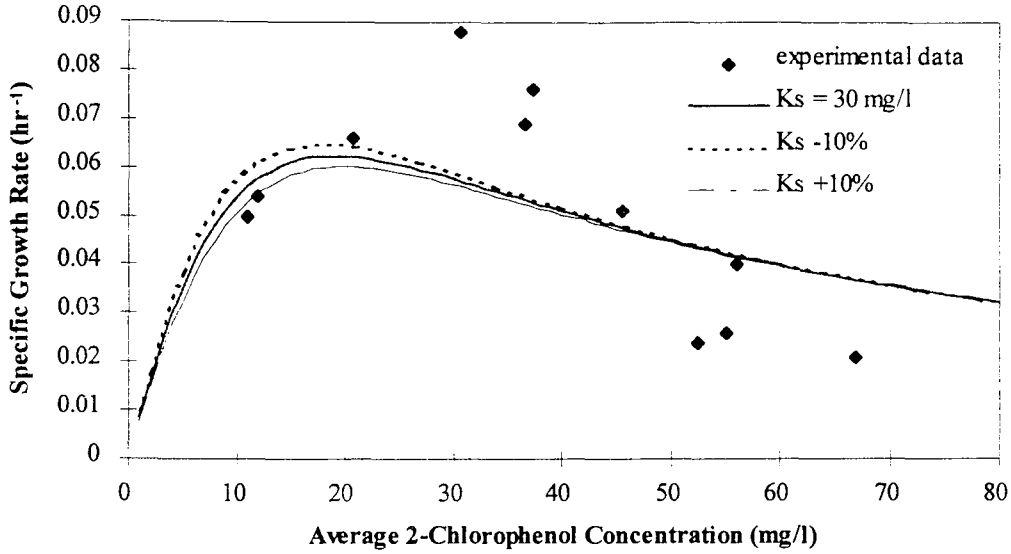

Figure A-31 Growth curve fit using estimated Andrews Model parameters showing results of perturbations of K_S.

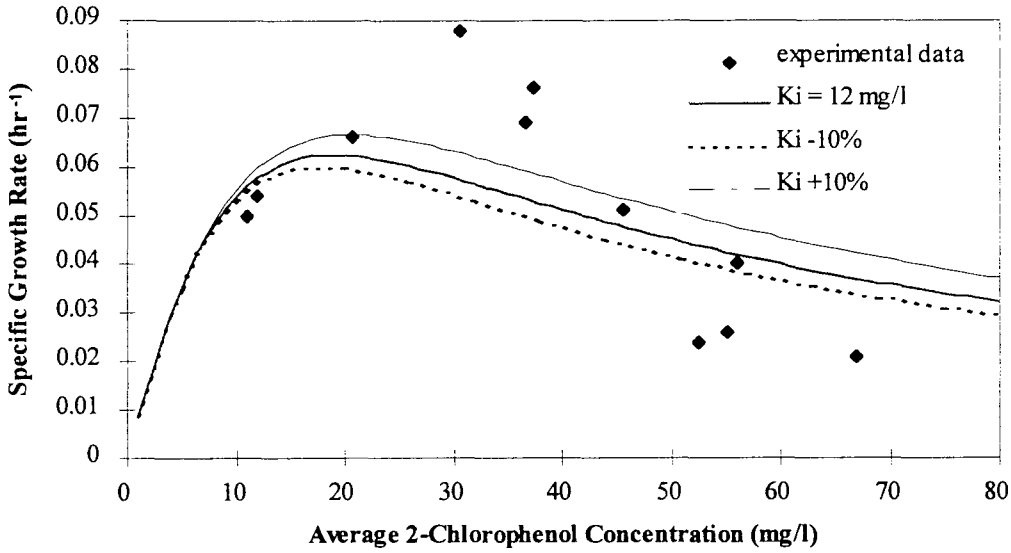

Figure A-32 Growth curve fit using estimated Andrews Model parameters showing results of perturbations of K_I.

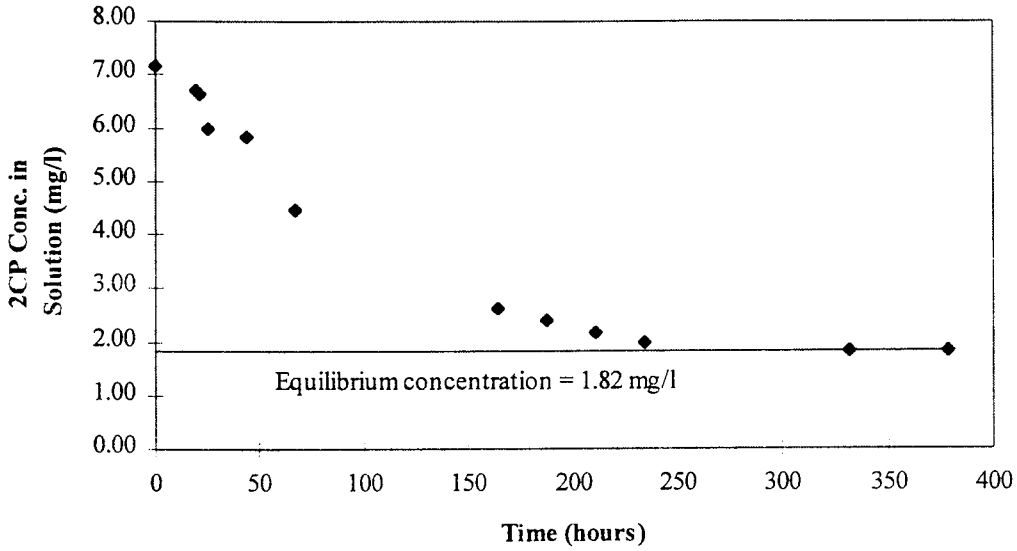

Figure A-33 2-chlorophenol concentration in solution as a function of time for the initial batch soil adsorption experiments.

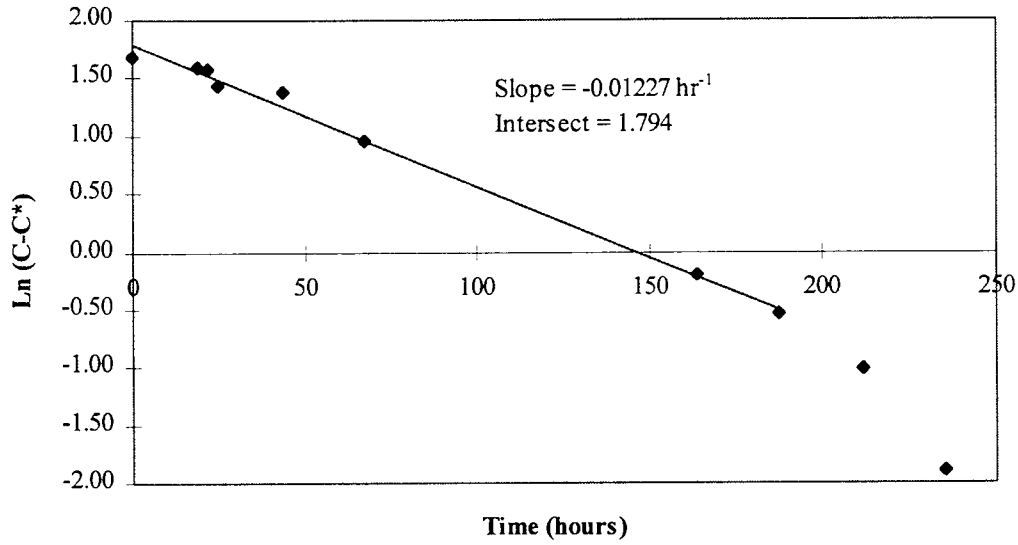

Figure A-34 Plot of ln(C-C*) versus time for the determination of adsorption parameters K_d and k'.

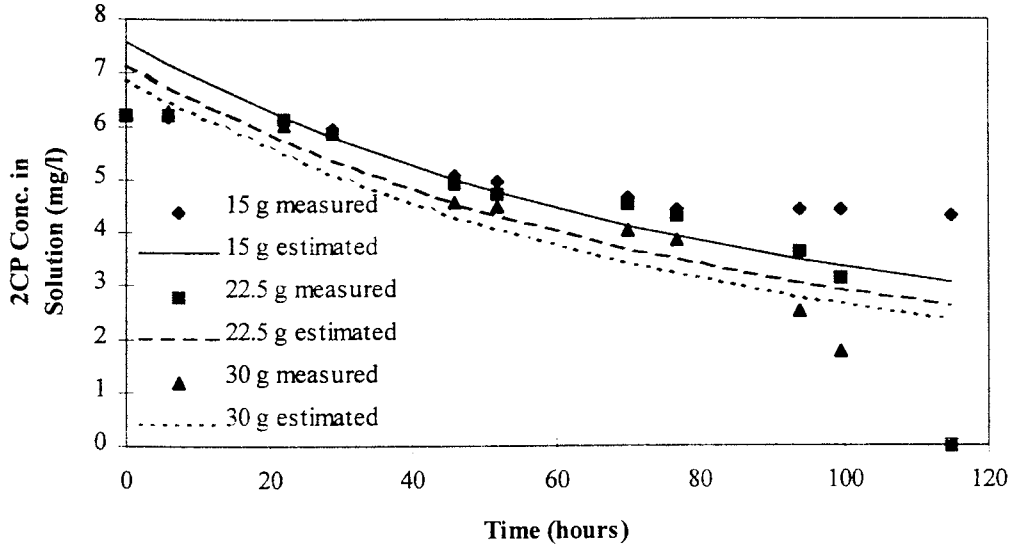

Figure A-35 2-chlorophenol concentration in solution as a function of time for the second batch of soil adsorption experiments.

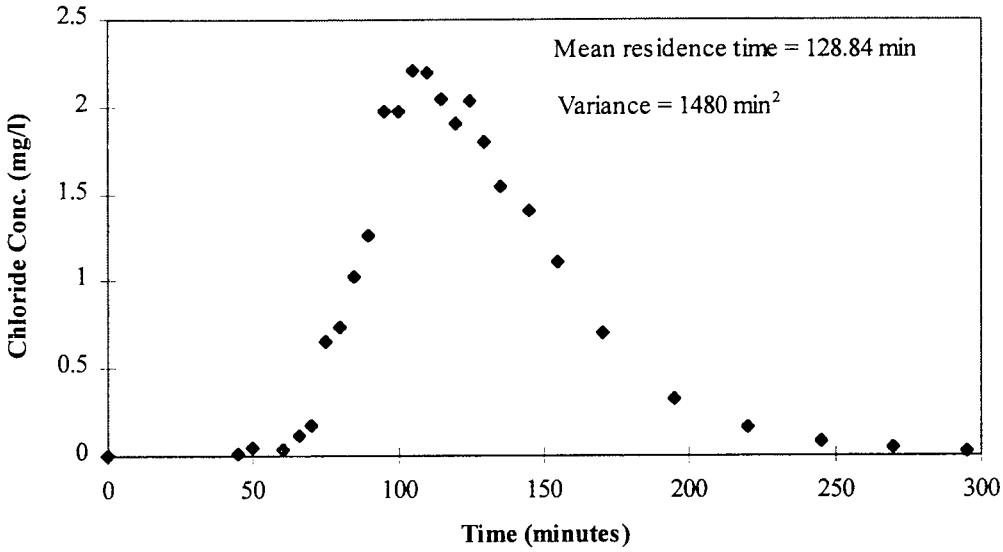

Figure A-36 Distribution of chloride detected at port 5 during chloride tracer study at flow rate 0.85 ml/min.

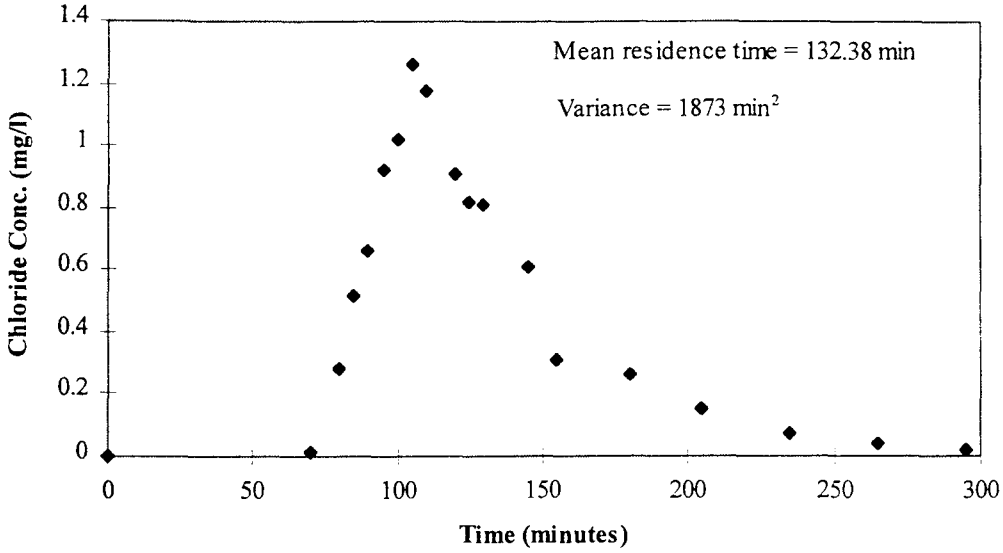

Figure A-37 Distribution of chloride detected at port 5 during chloride tracer study at flow rate 1.05 ml/min.

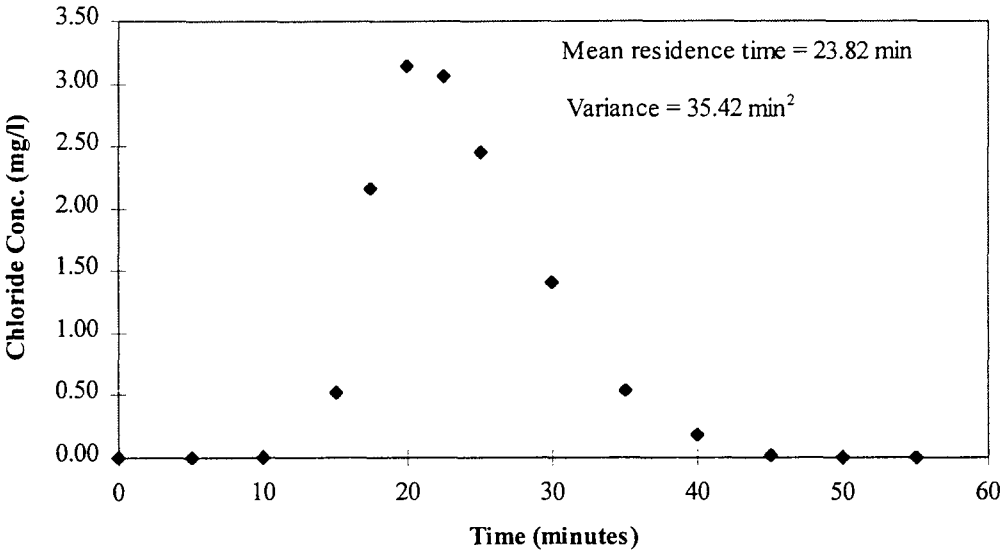

Figure A-38 Distribution of chloride detected at port 5 during chloride tracer study at flow rate 4.45 ml/min.

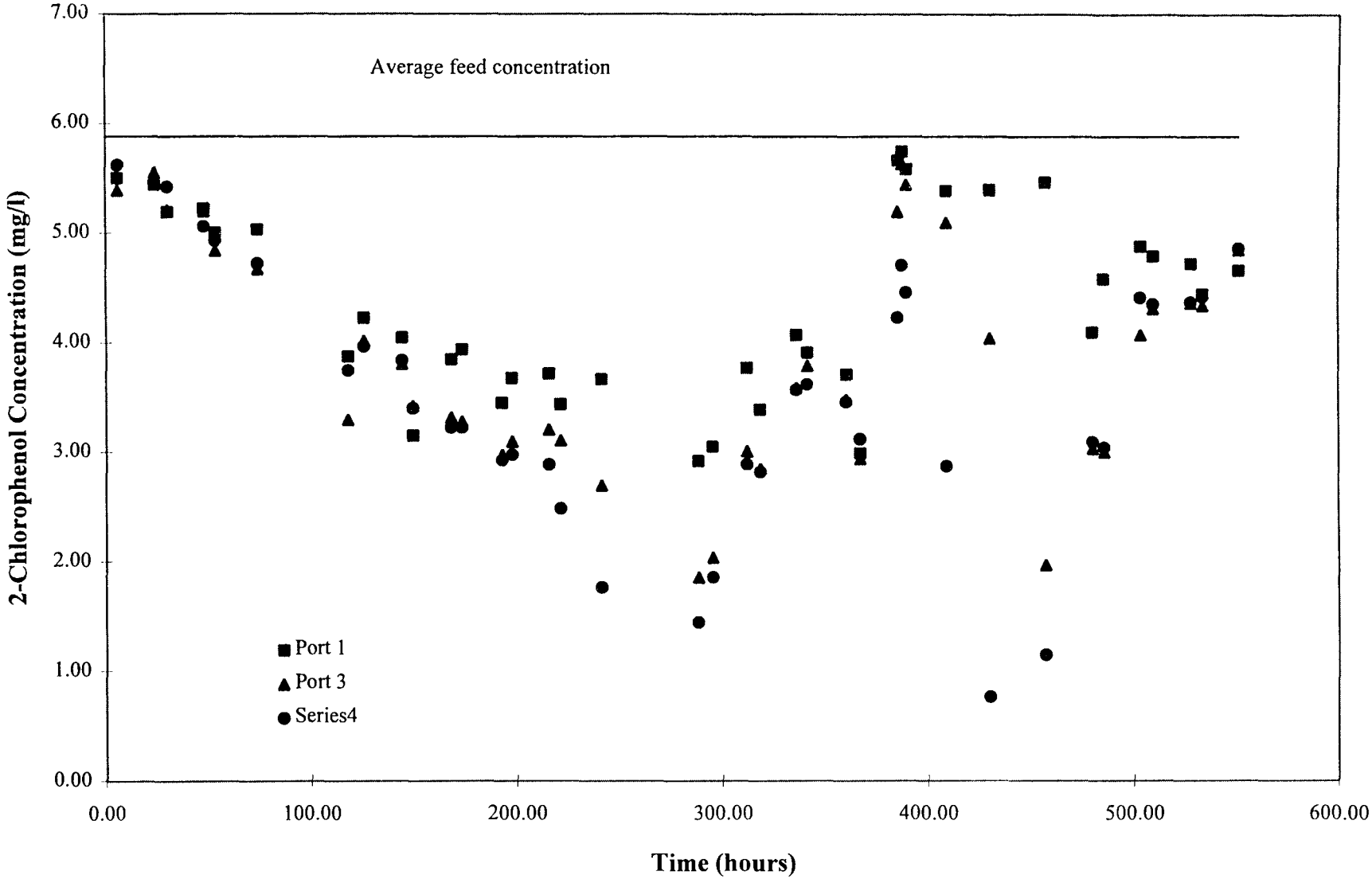

Figure 39 Concentration of 2-chlorophenol detected over time at column sampling ports - Data set 1

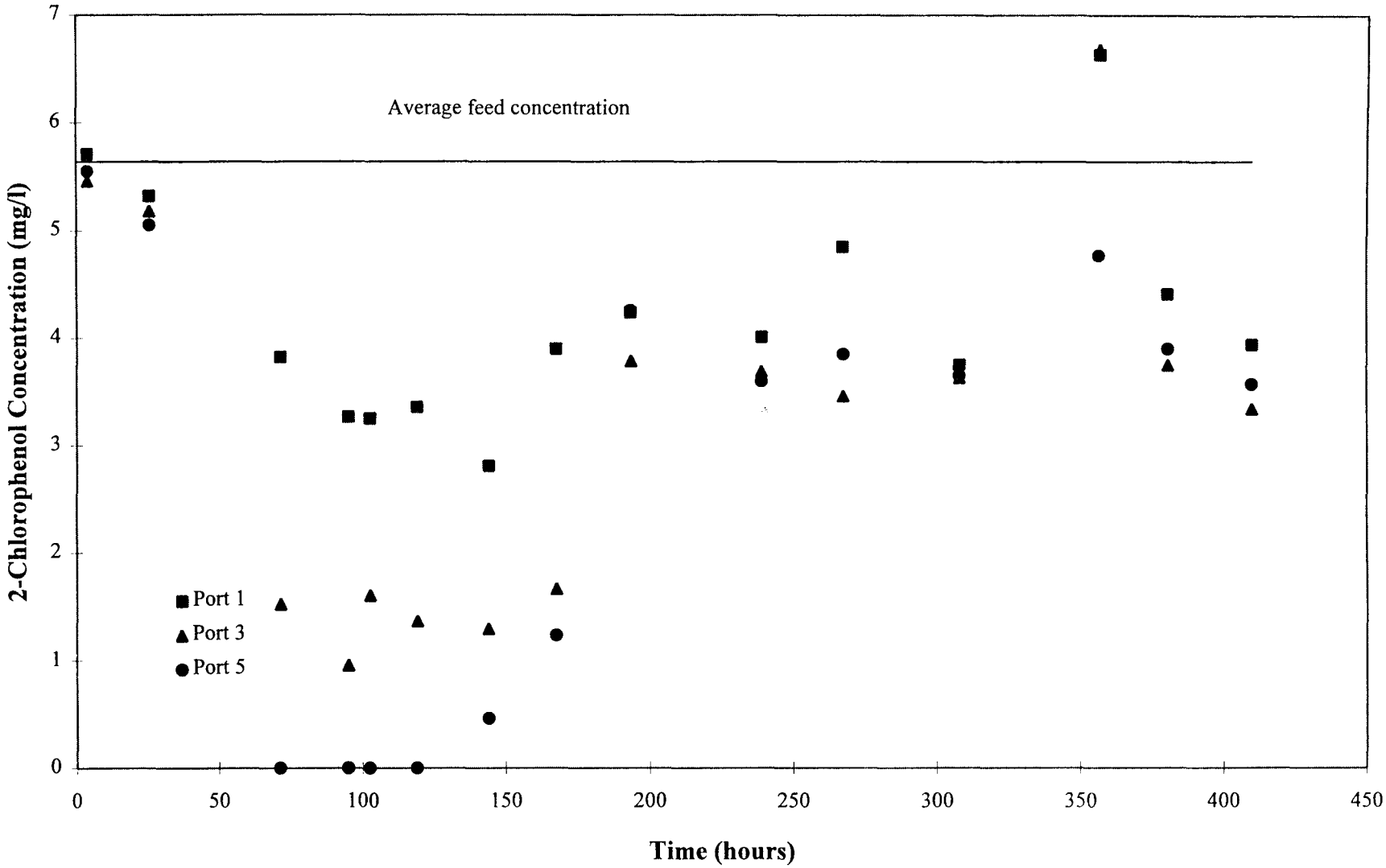

Figure 40 Concentration of 2-chlorophenol detected over time at column sampling ports - Data set 2

REFERENCES

Bahr, J. M. 1989. "Analysis of Nonequilibrium Desorption of Volatile Organics During Field Test of Aquifer Decontamination." *Journal of Contaminant Hydrology.* 4: 205-222.

Bakke, R. 1986. *Biofilm Detachment.* Ph.D. thesis. Montana State University, Bozeman, MT.

Barth, E.F., and C. C. Wiles. 1989. "Technical and Regulatory Status of Solidification/Stabilization in the United States." *Immobilization Technology Seminar.* EPA. CERI-89-222.

Borden, R. C., and P. B. Bedient. 1986. "Transport of Dissolved Hydrocarbons Influenced by Oxygen-Limited Biodegradation 1. Theoretical Development." *Water Resources Research.* 22: 1973-1982.

Borden, R. C., P. B. Bedient, M. D. Lee, C. H. Ward, and J. T. Wilson. 1986. "Transport of Dissolved Hydrocarbons Influenced by Oxygen-Limited Biodegradation 2. Field Application." *Water Resources Research.* 22: 1983-1990.

Borden, R. C., M. D. Lee, J. T. Wilson, C. H. Ward, and P. B. Bedient,. 1984. 'Modeling the Migration and Biodegradation of Hydrocarbons Derived from a Wood-Creosoting Process Waste." In *Proceedings of the NWWA/API Conference on Petroleum Hydrocarbons and Organic Chemicals in Ground Water - Prevention, Detection and Restoration.* National Water Well Association. 130-143.

Bouwer, E. J. 1992. "Microbial Remediation: Strategies, Potentials, and Limitations." *Proceedings of the European Conference on Integrated Research for Soil and Sediment Protection and Remediation.* Maastricht, The Netherlands. 1-11.

Crittenden, J. C., N. J. Hutzler, D. G. Geyer, J. L. Oravitz, and G. Friedman. 1986. "Transport of Organic Compounds with Saturated Groundwater Flow: Model Development and Parameter Sensitivity." *Water Resources Research.* 22: 271-284.

Dikshitulu, S. 1993. "Competition between two microbial populations in a sequencing fed-batch reactor and its implications for waste treatment." Ph.D. thesis. New Jersey Institute of Technology. Newark, NJ.

Domenico, P. A., and F. W. Schwartz. 1990. *Physical and Chemical Hydrogeology.* New York: John Wiley and Sons, Inc.

EPA Document: Innovative Treatment Technologies Status Report. EPA/540/2-91/002.

EPA Document: Innovative Treatment Technologies. EPA/540/9-91/002.

Esposito, P., J. Hessling, B. Locke, M. Taylor, M. Szabo, R. Thurnau, C. Rogers, R. Traver, and E. Barth. 1989. "Results of treatment evaluation of a contaminated synthetic soil." *J. Air Poll. Control Assoc.* 39: 294-304.

Hinchee, R. E., and R. F. Olfenbuttel, eds. 1991. *In-Situ Bioreclamation and On-Site Bioreclamation.* Butterwort-Heinemann, Boston, MA.

Kuhnt, G. 1990. "The Euro-Soil concept as a basis for chemicals testing and pesticide research." *Proceedings of the 3rd workshop on study and prediction of pesticides behavior in soils.* Munich, Germany.

Levenspiel, O. 1972. Chemical Reaction Engineering. Second Edition. New York: John Wiley and Sons, Inc.

McCarty, P. L., M. Reinhard, and B. E. Rittmann. 1981. "Trace Organics in Groundwater." *Environ. Sci. Technol.* 15: 40-51.

McCarty, P. L., B. E. Rittmann, and E. J. Bouwer. 1984. "Microbiological Processes Affecting Chemical Transformations in Groundwater." In *Groundwater Pollution Microbiology,* eds. G. Bitton and C. P. Gerba. Wiley Interscience, New York.

Ogram, A. V., R. E. Jessup, L. T. Ou, and P. S. Rao. 1985. "Effects of Sorption on Biological Degradation Rates of (2,4-Dichlorophenoxy) Acetic Acid in Soils." *Appl. Environ. Microbiol.* 49: 582-587.

Pickens, J. F., R. E. Jackson, K. J. Inch, and W. F. Merritt. 1981. "Measurement of Distribution Coefficients Using a Radial Injection Dual-Tracer Test." *Water Resources Research.* 17: 529-544.

Pignatello, J. J. 1989. "Sorption Dynamics of Organic Compounds in Soils and Sediments." Chapter 3 in *Reactions and Movements of Organic Chemicals in Soils.* Sawhney, B. L., and K. Brown, eds. Soil Science Society of America, Inc. and American Society of Agronomy, Inc. Madison, WI.

Rijnaarts, H. H., A. Bachmann, J. C. Jumelet, and A. J. Zehnder. 1990. "Effect of Desorption and Intraparticle Mass Transfer on the Aerobic Biomineralization of Hexachlorocyclohexane in a Contaminated Calcareous Soil." *Environ. Sci. Technol.* 24: 1349-1354.

Robinson, K. G., W. S. Farmer, and J. T. Novak. 1990. "Availability of Sorbed Toluene in Soils for Biodegradation by Acclimated Bacteria." *Water Resources.* 24: 345-350.

Scow, K. M., and J. Hutson. 1992. "Effect of Diffusion and Sorption on the Kinetics of Biodegradation: Theoretical Considerations." *Soil Sci. Soc. Am. J.* 56: 119-127.

Semprini, L., and P. L. McCarty. 1991. "Comparison Between Model Simulations and Field Results for In-situ Biorestoration of Chlorinated Aliphatics: Part 1. Biostimulation of Methanotrophic Bacteria." *Ground Water.* 29: 365-374.

Shuler, M. L., and F. Kargi. 1992. *Bioprocess Engineering: Basic Concepts.* New Jersey: PTR Prentice-Hall, Inc.

Srinivasan, P., and J. W. Mercer. 1988. "Simulation of Biodegradation and Sorption Processes in Groundwater." *Ground Water.* 26:475-487

Sykes, J. F., S. Soyupak, and G. J. Farquhar. 1982. "Modeling of Leachate Organic Migration and Attenuation in Groundwater Below Sanitary Landfills." *Water Resources Research.* 18: 135-145

Wu, S. C., and F. Gschwend. 1986. "Sorption Kinetics of Hydrophobic Organic Compounds to Natural Sediments and Soils." *Environ. Sci. Tech.* 20: 717-725.